

SEMI-ANNUAL REPORT

FOR

NASA Grant NAG-2-541

NASA Technical Monitor: Alex Woo

Institution: The Radiation Laboratory
Department of Electrical Engineering
and Computer Science
The University of Michigan
Ann Arbor, MI 48109-2122

Period Covered: September 1990 to February 1991

Report Title: Semi-Annual Report

Principal Investigator: John L. Volakis
Telephone: (313) 764-0500

enqn
UMR 0519

Preface

This semi-annual report describes our progress during the period from September 1990 to February 1991. Two specific tasks are described and each should be read independently. That is, figure and reference numbering is consecutive only within the description of the task. As can be expected the progress reports are very brief and the reader should refer to the referenced technical reports for detailed coverage. A total of 23 journal articles, 17 conference publications and 18 technical reports have been written since the beginning of the Grant. A complete list of these is given in pp. 40-45.

TABLE OF CONTENTS

	PAGE #
<u>TASK:</u> A FINITE ELEMENT CONJUGATE GRADIENT FFT METHOD FOR SCATTERING	2
Abstract	3
Objective	3
Background	4
Progress	5
Conclusions	6
Transitions	6
Figures	7-19
Appendix A	20
<u>TASK:</u> ANALYTICAL SOLUTIONS WITH GENERALIZED IMPEDANCE BOUNDARY CONDITIONS	28
Abstract	29
Objective	29
Progress	30
1. introduction	30
2. numerical results	31
Summary	32
References	32
Figures	35-39
Paper written (to date) under this grant	40
Conference papers presented/written to date	42
Reports written to date under this grant	44

Task Title **A Finite Element Conjugate
Gradient FFT Method for
Scattering**

Investigators **J.D. Collins, Dan Ross,
J.M.-Jin, A. Chatterjee and
J.L. Volakis**

Period Covered **Sept. 1990 - Feb. 1991**

ABSTRACT

Validated results are presented for the new 3D body of revolution finite element-boundary integral code. As usual, a Fourier Series expansion of the vector electric and magnetic fields is employed to reduce the dimensionality of the system and the exact boundary condition is employed to terminate the finite element mesh. The mesh termination boundary is chosen such that it leads to convolutional boundary operators for low $O(n)$ memory demand. Improvements of this code are discussed along with the proposed formulation for a full 3D implementation of the finite element-boundary integral method in conjunction with a CGFFT solution.

OBJECTIVE

The objective of this task is to develop innovative techniques and related software for scattering by three dimensional composite structures. The proposed analysis is a hybrid finite element-boundary integral method formulated to have an $O(n)$ memory demand. This low storage is achieved by employing the FFT to evaluate all boundary integrals and by resorting to an iterative solution algorithm. Particular emphasis in this task is the generation of software applicable to airborne vehicles and the validation of these by comparison with measured and other reference data. Because the approach is new, a step by step development procedure has been proposed over a three-year period. During the first year the technique was developed and implemented for two-dimensional composite structures. Support software for the two-dimensional analysis such as pre- and post-processor routines were developed during the second year and a formulation was also developed and implemented for three-dimensional bodies of revolution. Finally, during the third year, we will develop, implement, and test the method for arbitrary three dimensional structures.

BACKGROUND

Interest in three-dimensional (3-D) methods has increased in recent years, however, the associated demands in computation time and storage are often prohibitive for electrically large 3-D bodies. Vector and concurrent (i.e. hypercube, connection, etc.) computers are beginning to alleviate the first of these demands, but a minimization of the storage requirements is essential for treating large structures.

The traditional Conjugate Gradient Fast Fourier Transform (CGFFT) method [1] - [4] is one such frequency domain solution approach which requires $O(n)$ storage for the solution on n equations. This method involves the use of FFTs whose dimension equals that of the structure under consideration [5] - [7] and, therefore, demands excessive computation time when used in an iterative algorithm. Also, the standard CGFFT requires uniform rectangular gridding that unnecessarily includes the impenetrable portions of the scatterer. With these issues in mind, a new solution approach is proposed for solving scattering problems. The proposed method will be referred to as the Finite Element-Conjugate Gradient Fast Fourier Transform (FE-CGFFT) method.

During last year's effort the FE-CGFFT method was developed for two-dimensional scatterers where the finite element mesh was terminated at a rectangular box. Inside the box boundaries, Helmholtz equation is solved via the finite element method and the boundary constraint is obtained by an appropriate integral equation which implicitly satisfies the radiation condition. Along the parallel sides of the box, this integral becomes a convolution and is, therefore, amenable to evaluation via the FFT. The dimension of the required FFT in this hybrid method is one less than the dimensionality of the structure thus, making it attractive for 3-D simulations. Also, because it incorporates the finite element method, the FE-CGFFT formulation remains valid regardless of the structure's geometry and material composition.

The proposed method described in the University of Michigan Report 025921-6-T (see also [8]) is similar to the moment method version developed by Jin [9]. Jin's method was in turn based on work published in the early 70's by McDonald and Wexler [10] who introduced an approach to solve unbounded field problems. The proposed method is also similar to other methods (a few of which will be mentioned here), neither of which provides a storage reduction comparable to the proposed FE-CGFFT method. The unimoment method [11] uses finite elements inside a fictitious circular boundary and an eigenfunction expansion to represent the field in the external region. The coefficients of the expansion are then determined by enforcing field continuity at the finite element (FE) mesh boundary. The coupled finite element-boundary element method [12] uses the finite element method within the boundary and the boundary element method to provide the

additional constraint at the termination of the mesh. Unlike the proposed method, the solution in [12] was accomplished by direct matrix inversion (as in [9]), and the outer mesh boundary is not rectangular to take advantage of the FFT for the evaluation of the boundary integrals.

PROGRESS

Part of our efforts in this task were devoted to debugging and validating the three dimensional body of revolution (BOR) code developed in the previous months. The analysis associated with this code is described in the U of M technical report 025921-18-T where we also include validation data obtained over the past two months. Some of these are shown in figures 1-3 and refer to an ogive, a circular cylinder and a sphere. Unfortunately, it was found that as the bodies became larger the system's condition deteriorates and this was traced to the pulse basis formulation employed for the discretization of the boundary. Through several tests we have now shown that A Galerkin's linear basis formulation will correct the convergence difficulties. For example, this formulation was already employed in solving large systems (with more than 120,000 unknowns) associated with the scattering by frequency selective surfaces (FSS) and large Mates. As shown in figure 4-5, the Galerkin's formulation with linear basis permitted a solution of this system in less than 70 iterations! In comparison, the pulse basis-point matching formulation would require several thousand iterations before reaching convergence. Consequently, we are in the process of incorporating the Galerkin's linear basis formulation into our existing 2D and 3D BOR codes. Further, it was found that the ech area converges much sooner than the mean square error and permitted us to speed-up solution time.

During this last quarter we also began the development of the proposed finite element formulation for general non-symmetric inhomogeneous bodies. The basic discrete elements in this case are tetrahedra in conjunction with edge-based expansion functions. The associated finite element formulations is described in Appendix A and we are now in the process of implementing it. Initially, the finite element mesh will be terminated by a fictitious absorbing layer whose dielectric parameters were determined by a minimization of the reflection coefficient over the entire range of incidence angles. For a three layer coating, each of thickness 0.05 wavelengths, it was found that their respective dielectric properties to minimize the reflection coefficient over all angles of incidence are

$$\begin{aligned}\epsilon_{r1} &= (-0.1249205, -1.731605), \mu_{r1} = (-1.031792, -0.1039932) \\ \epsilon_{r2} &= (0.040699530, 0.1750280), \mu_{r1} = (0.3155941, 0.3190330) \\ \epsilon_{r3} &= (-1.278644, 0.9625375), \mu_{r3} = (-0.1721315, -5.389832)\end{aligned}$$

The corresponding plot of the reflection coefficient as a function of incidence is given in figure 7 along with scattering patterns based on the proposed termination model. As seen, for the chosen fictitious absorber the reflection coefficient is less than one percent for θ up to 62 degrees and less than 2 percent for θ up to 77 degrees. For the same error criteria, the corresponding angles associated with the second order Padé ABC are 35 and 41 degrees, respectively. The fictitious ABC has, therefore, a substantially better performance over the existing ABCs, and its effectiveness will be examined further in the next few months.

The three dimensional finite element meshes required in the analysis will be generated by SDRC IDEAS and we have already began to develop the software for transforming the output of this commercial package to the input files of our analysis codes. Similar drivers were already developed for the two dimensional code which was developed last year.

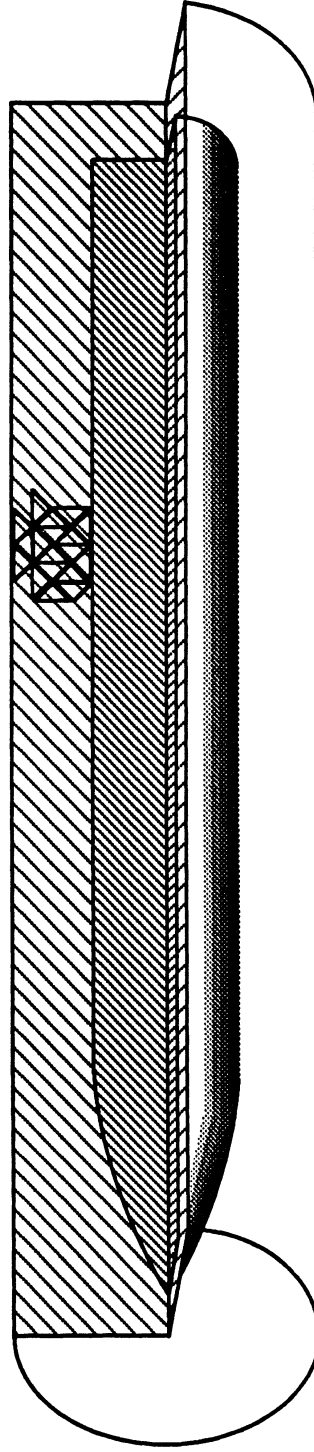
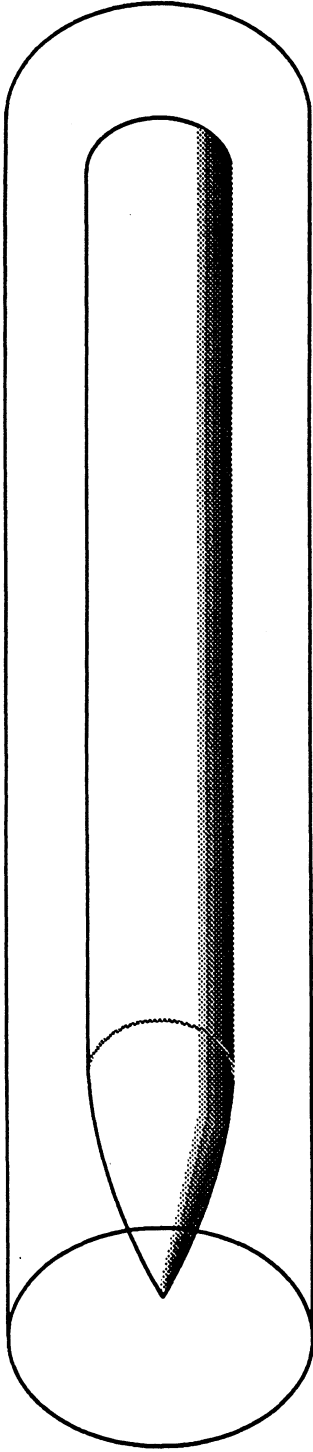
Finally, during this period we performed extensive testing of the two-dimensional code and have in the progress developed several new pre- and post- processing algorithms for this code. Two of the new geometries (see fig. 8 and 11) whose scattering was computed with our 2D finite element - CGFFT code are displayed in figures 9, 11 and 12. These represent airfoil configurations, one of which is coated with a dielectric material.

CONCLUSIONS

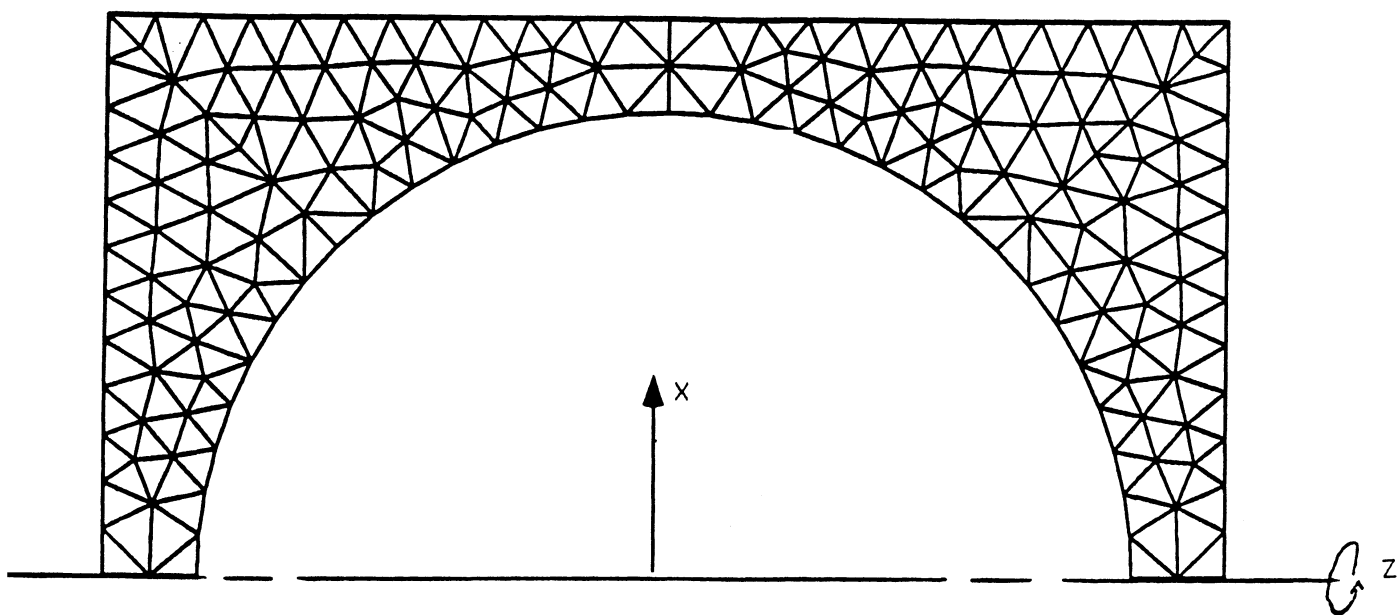
The project continues to evolve in accordance with our original plan and schedule. Most importantly, so far, our expectation of the finite element CGFFT formulation have been realized and we are, therefore, pleased with its performance for the intended applications.

TRANSITIONS

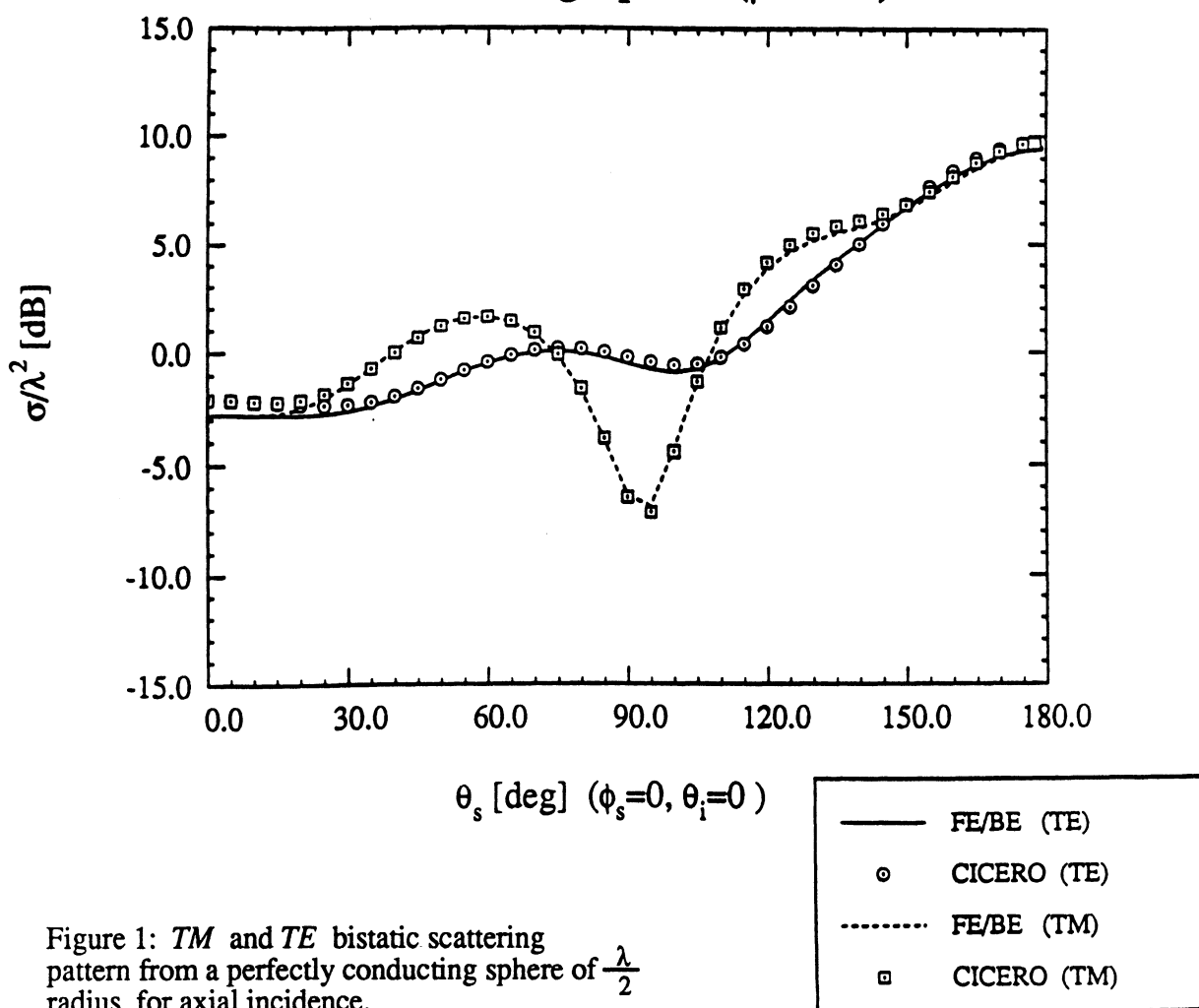
All of our efforts in the next six months will be devoted to the development of the 3D finite element boundary integral code for arbitrary structures. In the immediate future we will also pursue improvements for our existing codes primarily directed at speeding the convergence of the CG or BiCG algorithm.



Body of Revolution enclosed in a fictitious finite length cylinder. Area between the Scatterer and the fictitious cylinder is discretized via the finite element method.



Conducting Sphere ($\rho=0.5\lambda$)



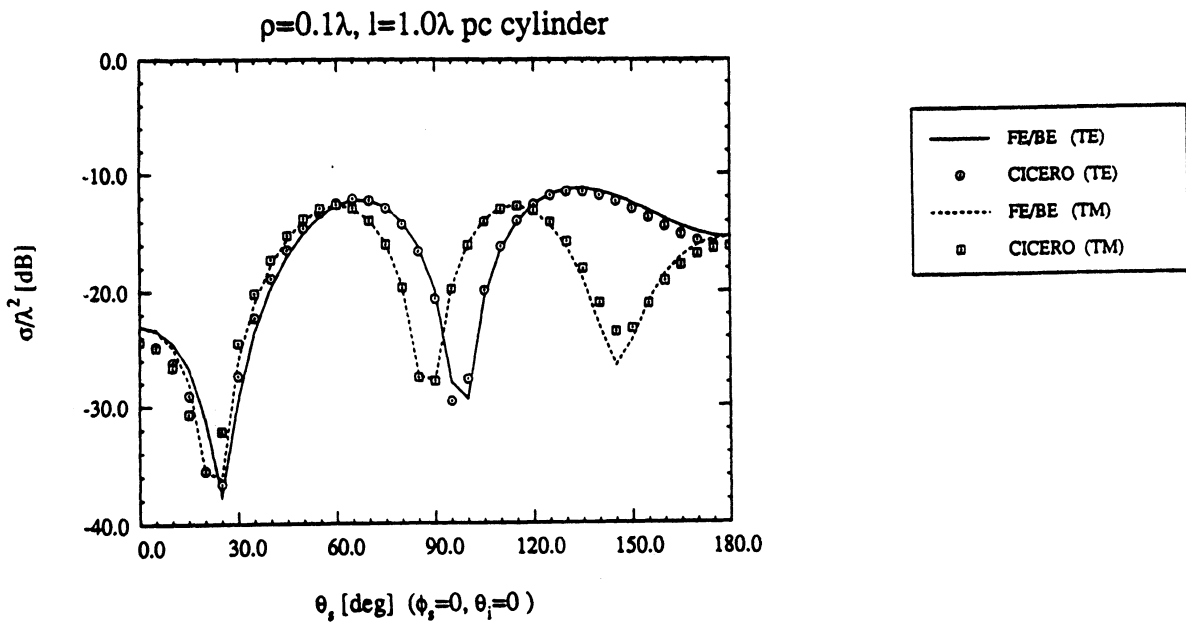
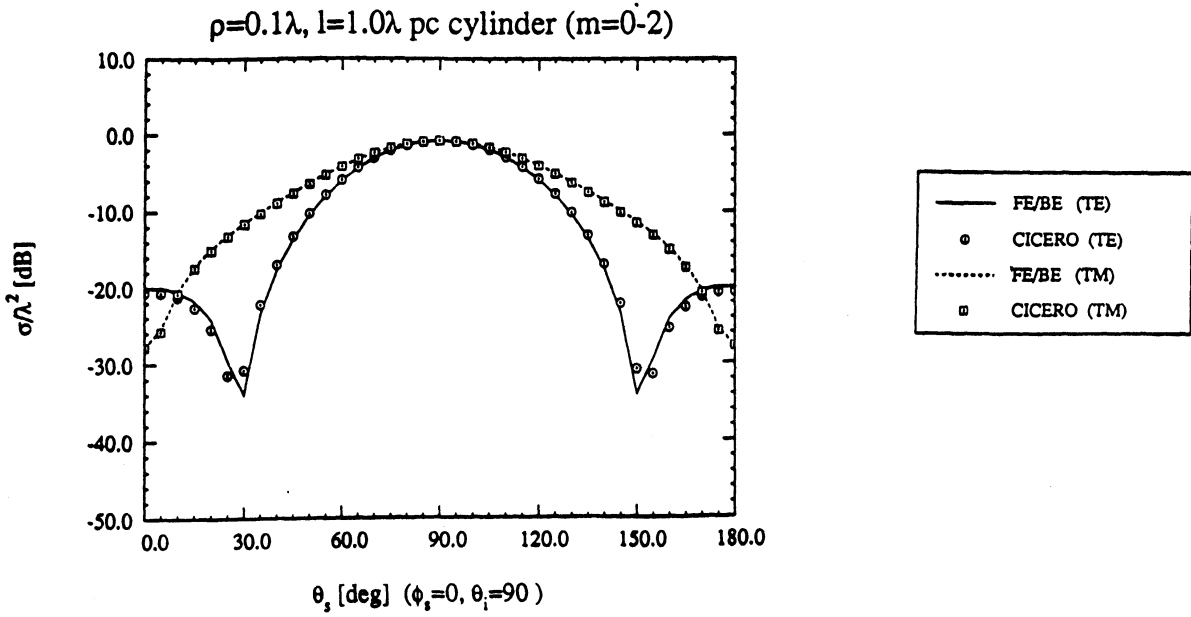
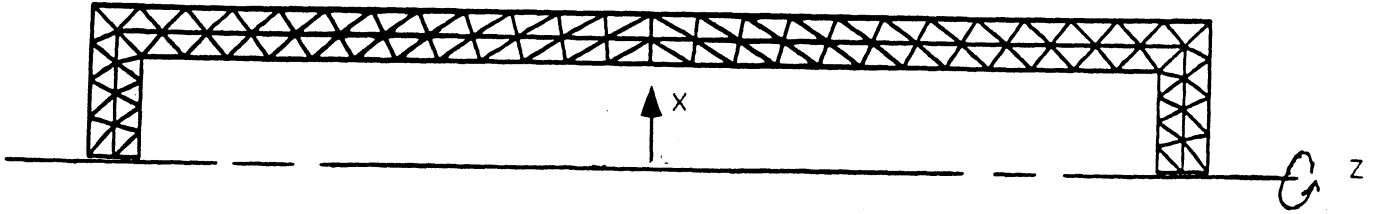


Figure 2: *TM* and *TE* bistatic scattering pattern from a perfectly conducting circular cylinder of length 1λ and radius 0.1λ for axial incidence. (a) modes 0-2, (b) converged

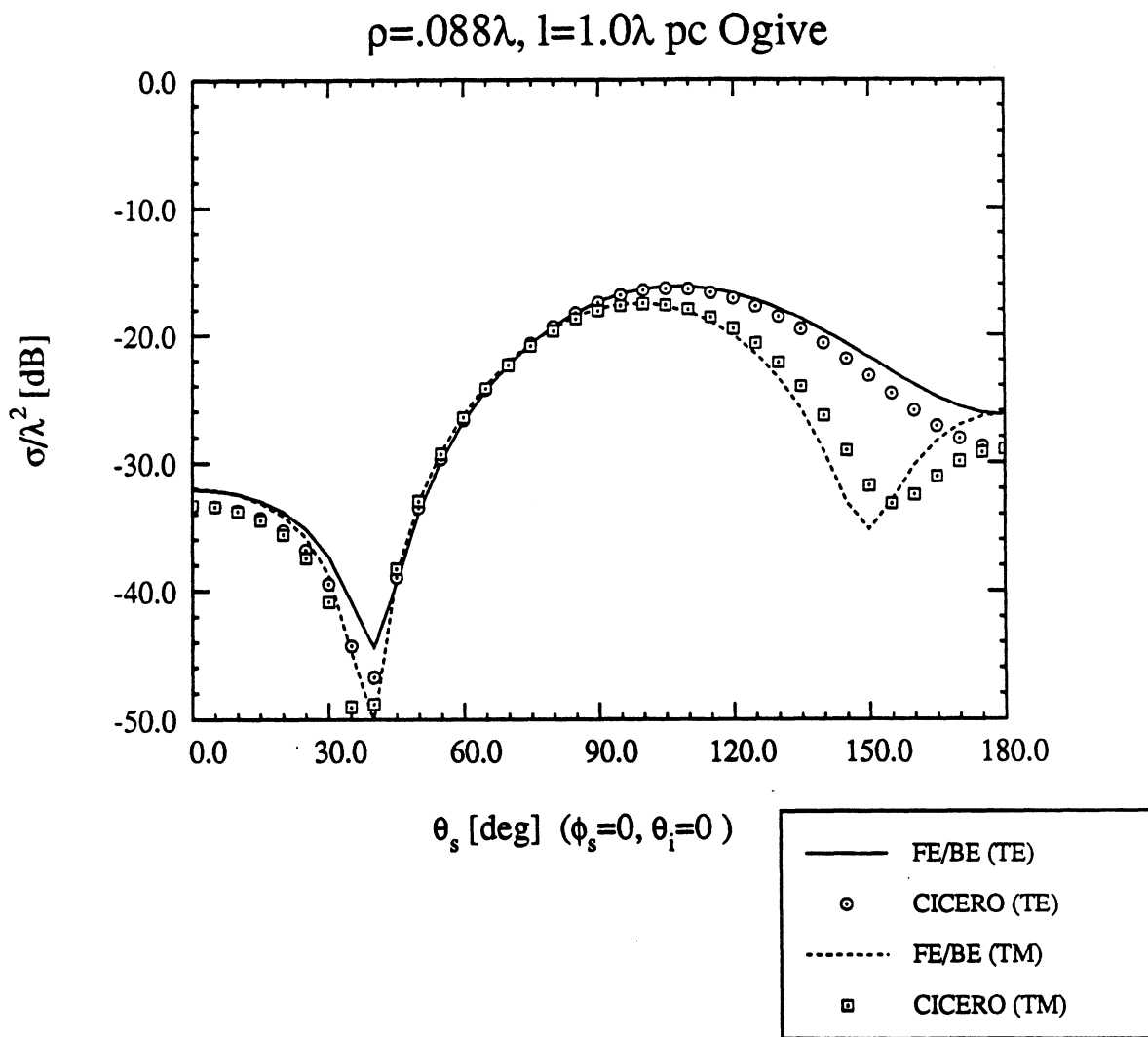
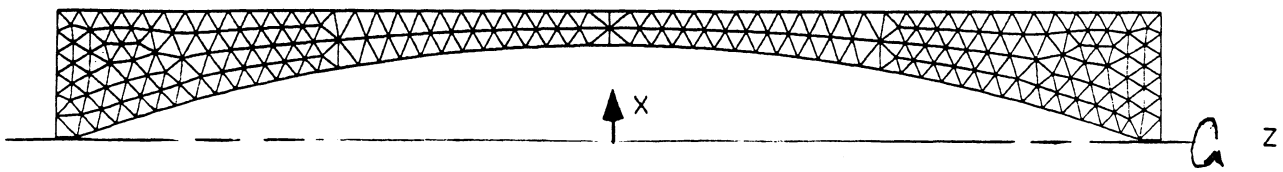


Figure 3: *TM* and *TE* bistatic scattering pattern from a perfectly conducting ogive length 1λ and maximum radius of 0.088λ for axial incidence.

FSS ARRAY SCATTERING

12 x 12 FSS Array

f=24 GHz

$\phi_{inc} = 45^\circ$ $\theta_{inc} = 75^\circ$

28,084 Unknowns

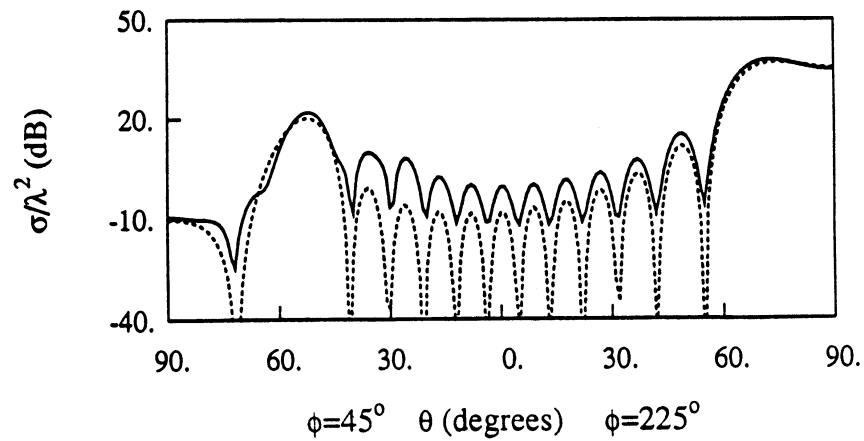
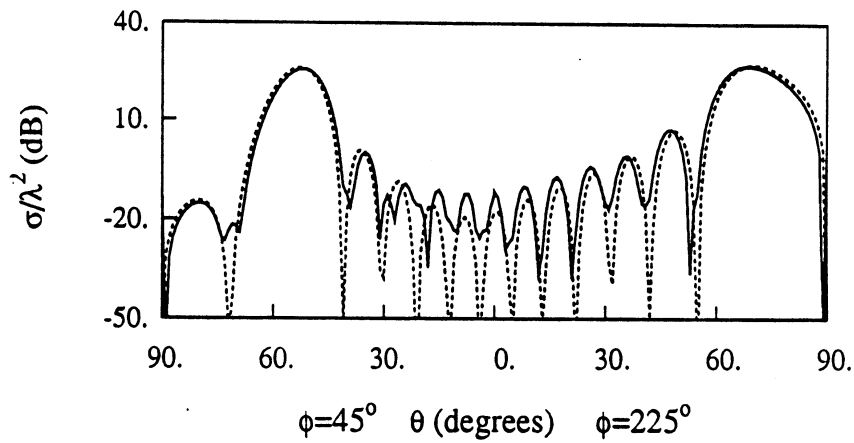
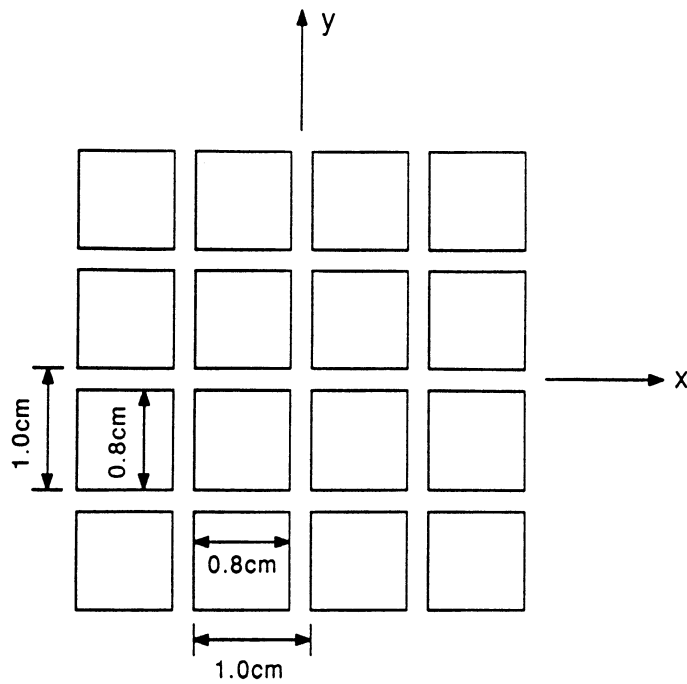


Figure 4: Scattering by a 12 x 12 FSS array; comparison of the exact solution (solid line) with an approximate result obtained by truncating the infinite FSS.

FSS ARRAY SCATTERING

24 x 24 FSS Array

f=24 GHz

$\phi_{inc} = 0^\circ$ $\theta_{inc} = 45^\circ$

123,504 Unknowns

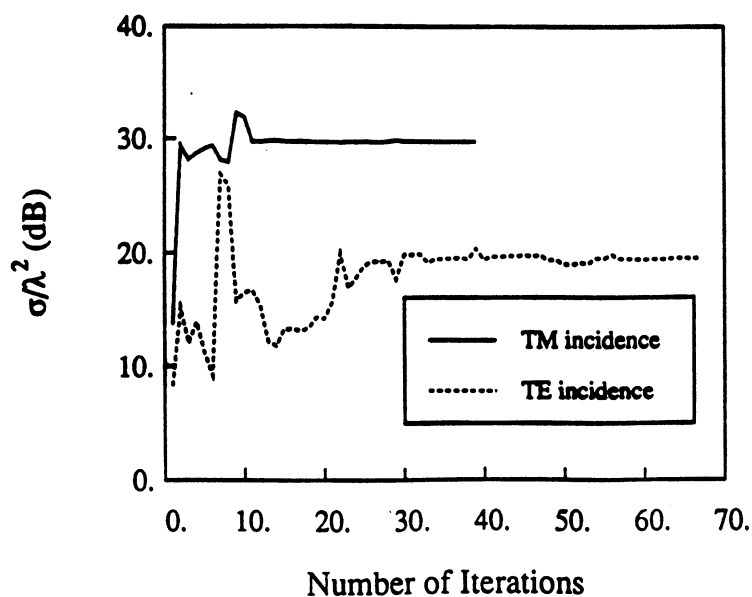
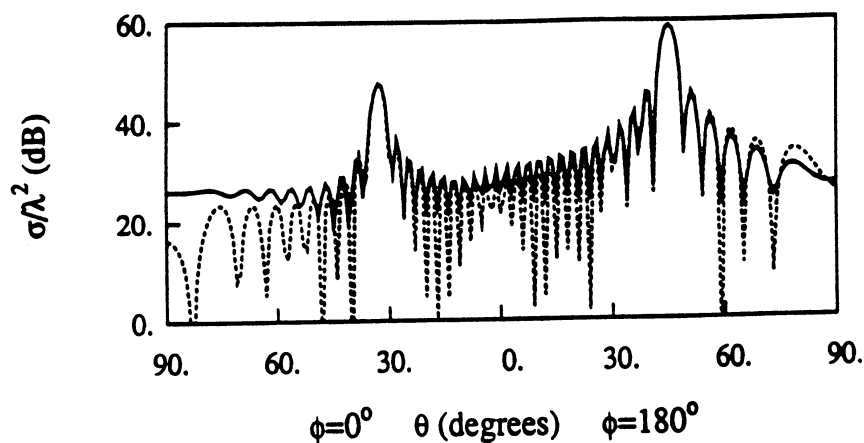
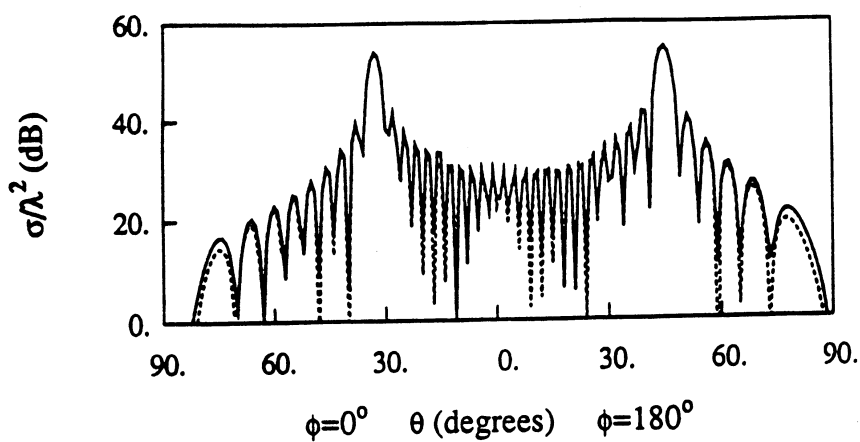
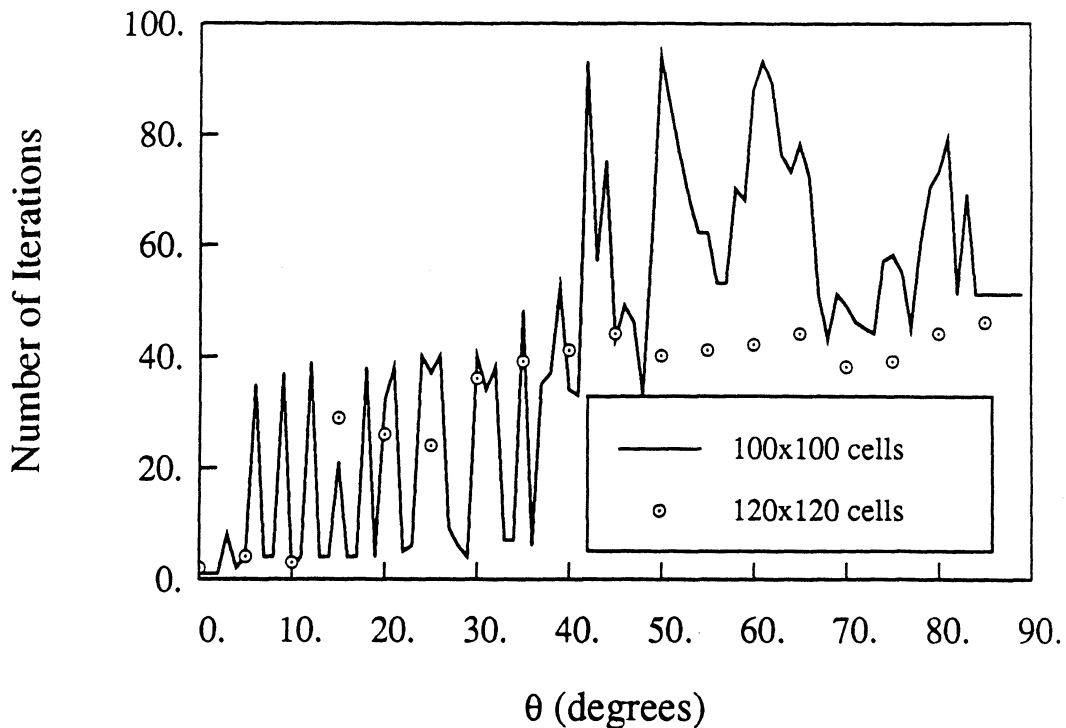


Figure 5: Scattering by a 24 x 24 array; comparison of the exact solution (solid line) with an approximate result obtained by truncating the infinite FSS.

LARGE PLATE SCATTERING

Principal Plane Cut

$10\lambda \times 10\lambda$ plate, TM incidence, BiCG-FFT



$10\lambda \times 10\lambda$ plate, TM incidence, BiCG-FFT

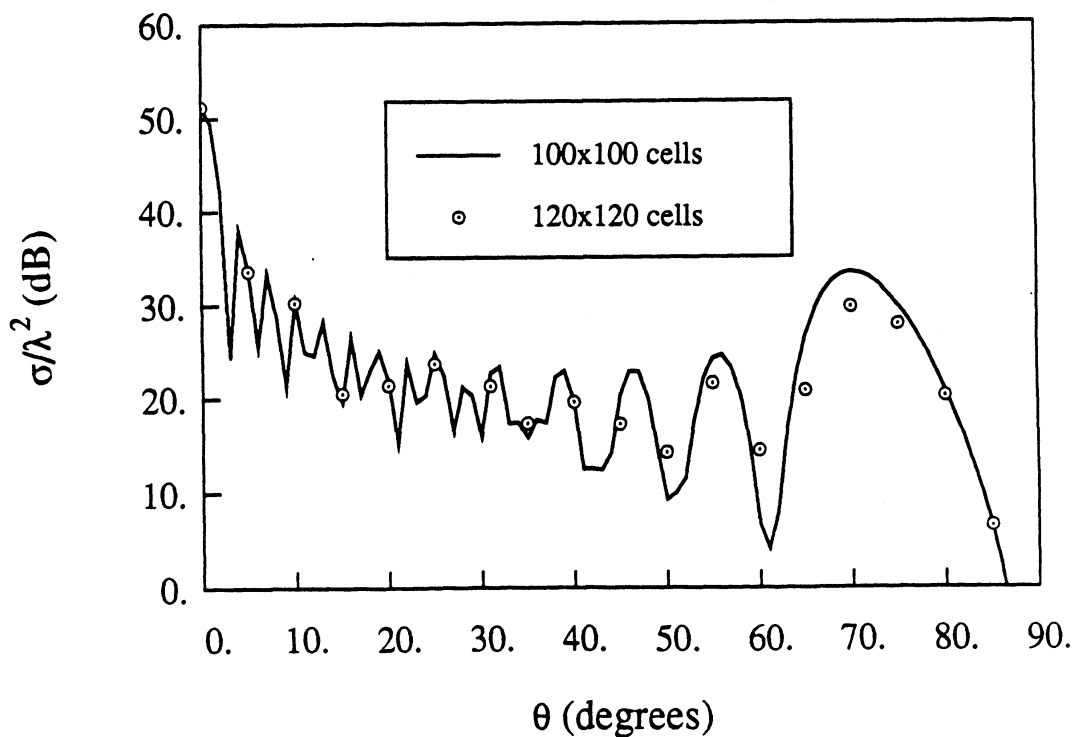


Figure 6: Principal plane *TM* Scattering by a $10\lambda \times 10\lambda$ rectangular plate.

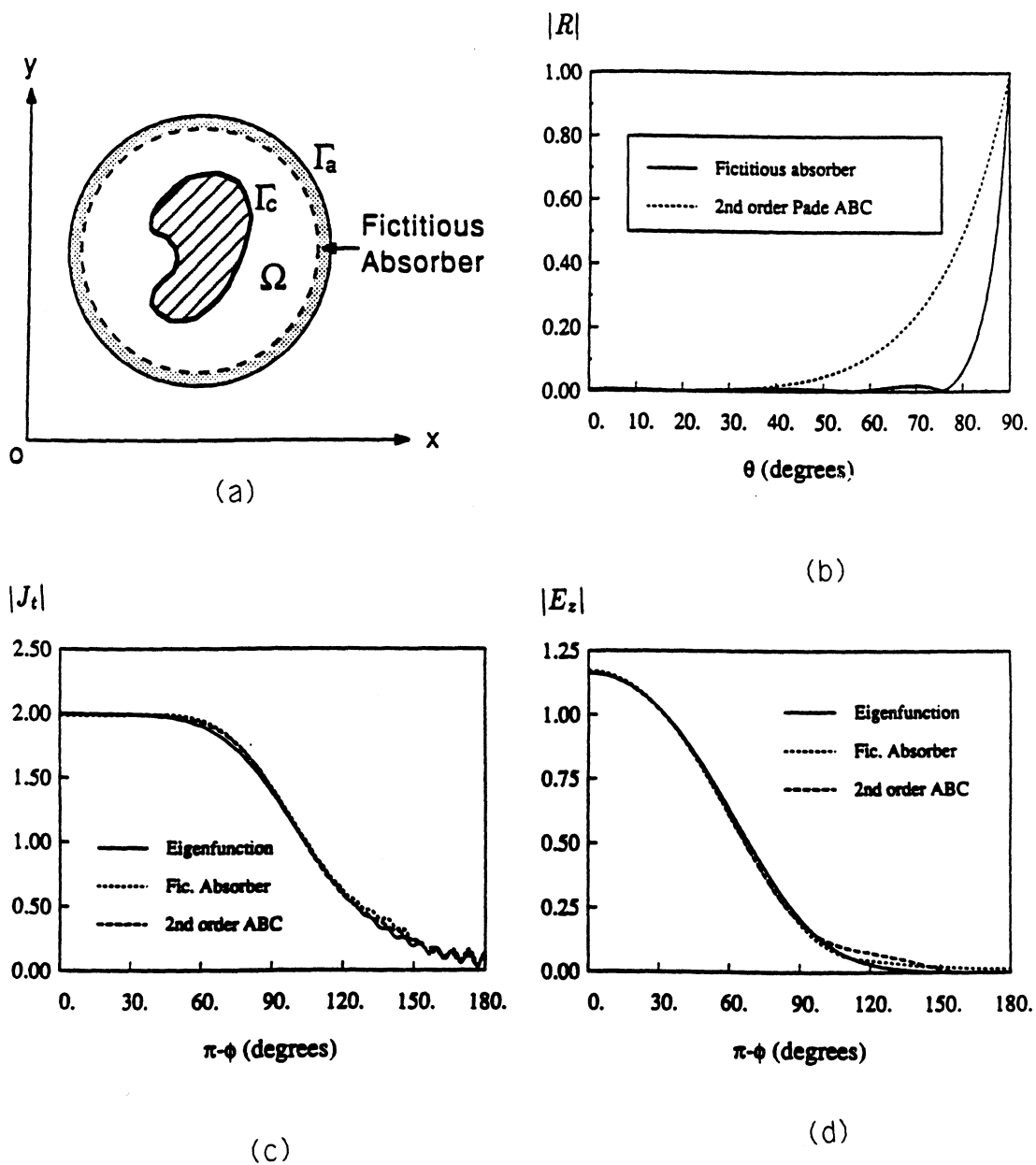


Figure 7: Evaluation of the new fictitious ABC (a) geometry (b) reflection coefficient plot (c) H_z field on a PEC Circular Cylinder (d) E_z field at a distance $\lambda/10$ from the surface of a PEC Circular Cylinder.

case 2: Coated Trailing Edge

$$y_{\text{in}} = \begin{cases} \pm \frac{1}{2} \sqrt{1 - (x/2.5)^2} & -2.5 \leq x \leq 0 \\ \pm 0.8232 A(x) & 0 \leq x \leq 2.5 \end{cases}$$

$$A(x) = \sqrt{\left(1 - (x/2.7182)^2\right)} - 0.3926$$

$$y_{\text{out}} = \pm 0.8116 B(x) \quad 0.1 \leq x \leq 3.0$$

$$y_{\text{out}} = y_{\text{in}} \quad \text{elsewhere}$$

$$B(x) = \sqrt{1 - [(x-.1)/3.1416]^2} - .3846$$

$$\epsilon_r = 2 - j1 \quad \text{between } y_{\text{in}} \text{ and } y_{\text{out}}$$

FEM Mesh

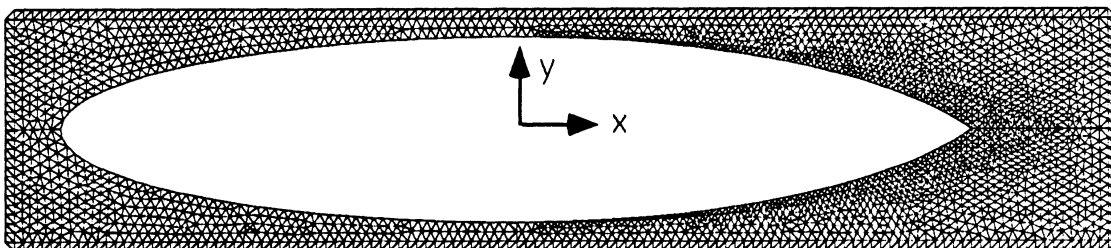
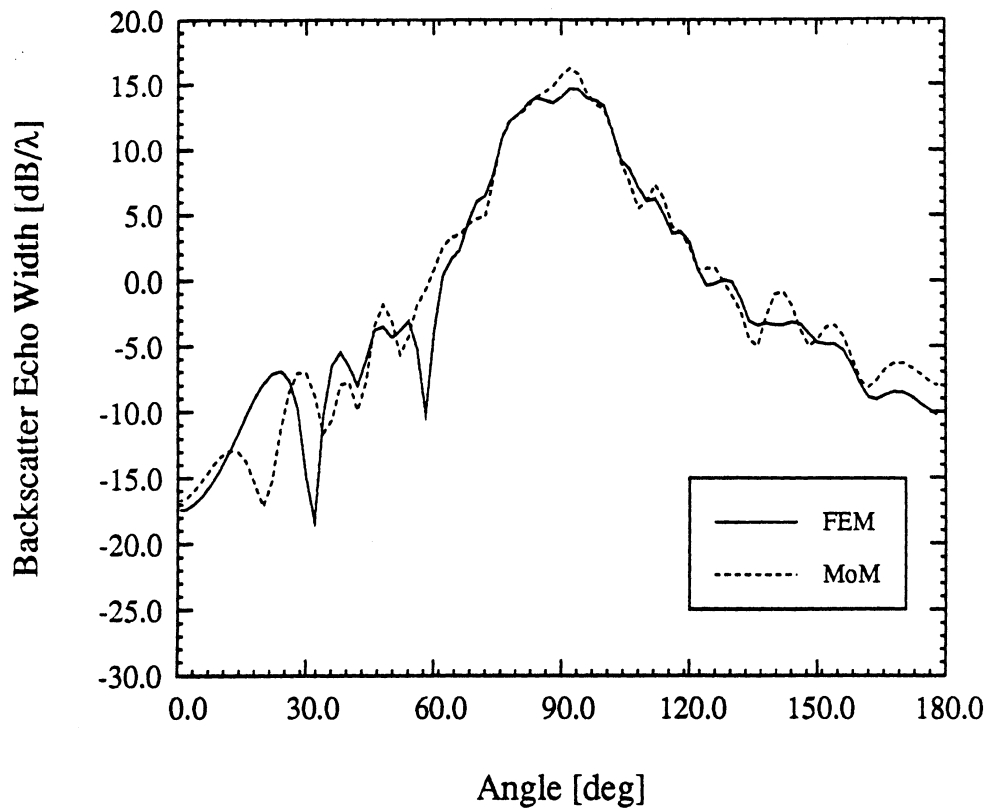


Figure 8: Geometry and finite element mesh of the illustrated coated trailing edge

Case 2: Coated trailing edge, ($\epsilon=2-j1$), H-pol



Case 2: Coated trailing edge, ($\epsilon=2-j1$), E-pol

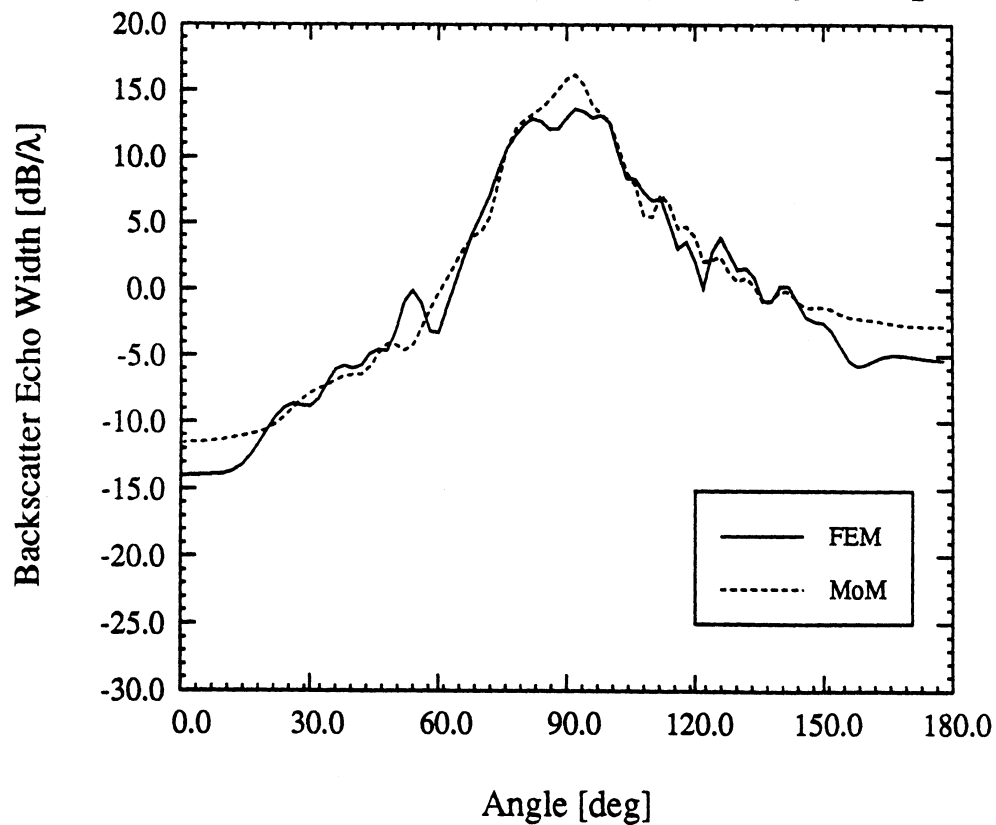
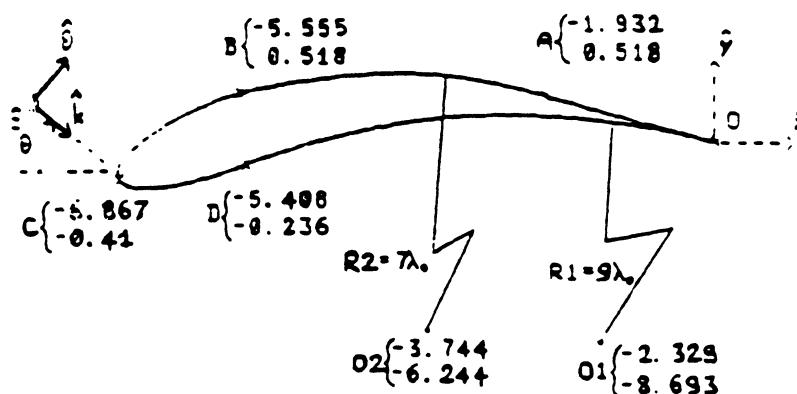


Figure 9: E and H polarization scattering patterns for the configuration shown in figure 8. Comparison of results between the FE-CGFFT and the moment method.

Perfectly conducting airfoil

All dimensions in wavelengths. The airfoil section is made by 5 arcs:



- OA : straight line
- AB : circle of radius $R2 = 7\lambda_0$ and of center O2
- BC : polynomial parametric equation
- CD : polynomial parametric equation
- DO : circle of radius $R1 = 9\lambda_0$ and of center O1

The polynomial equation are given by:

$$x(u) = \sum_{i=1}^6 a_i \cdot u^{(i-1)} \quad y(u) = \sum_{i=1}^6 b_i \cdot u^{(i-1)} \quad 0 \leq u \leq 1$$

a_i and b_i for BC arc

a_i and b_i for CD arc

$a_1 = 4.61149$	$b_1 = 1.53278$	$a_1 = -1.62131$	$b_1 = -0.12563$
$a_2 = -12.11403$	$b_2 = -3.22680$	$a_2 = 4.54389$	$b_2 = 0.30612$
$a_3 = 8.88606$	$b_3 = 0.90615$	$a_3 = -3.32901$	$b_3 = 0.16113$
$a_4 = 0.44275$	$b_4 = 1.24623$	$a_4 = 0.35663$	$b_4 = -0.00343$
$a_5 = -0.51440$	$b_5 = 0.46927$	$a_5 = -1.40984$	$b_5 = -0.51216$
$a_6 = -6.86720$	$b_6 = -0.41007$	$a_6 = -5.40756$	$b_6 = -0.23609$

Figure 10: Geometry of a PEC Airfoil whose scattering is given in figures 11 & 12.

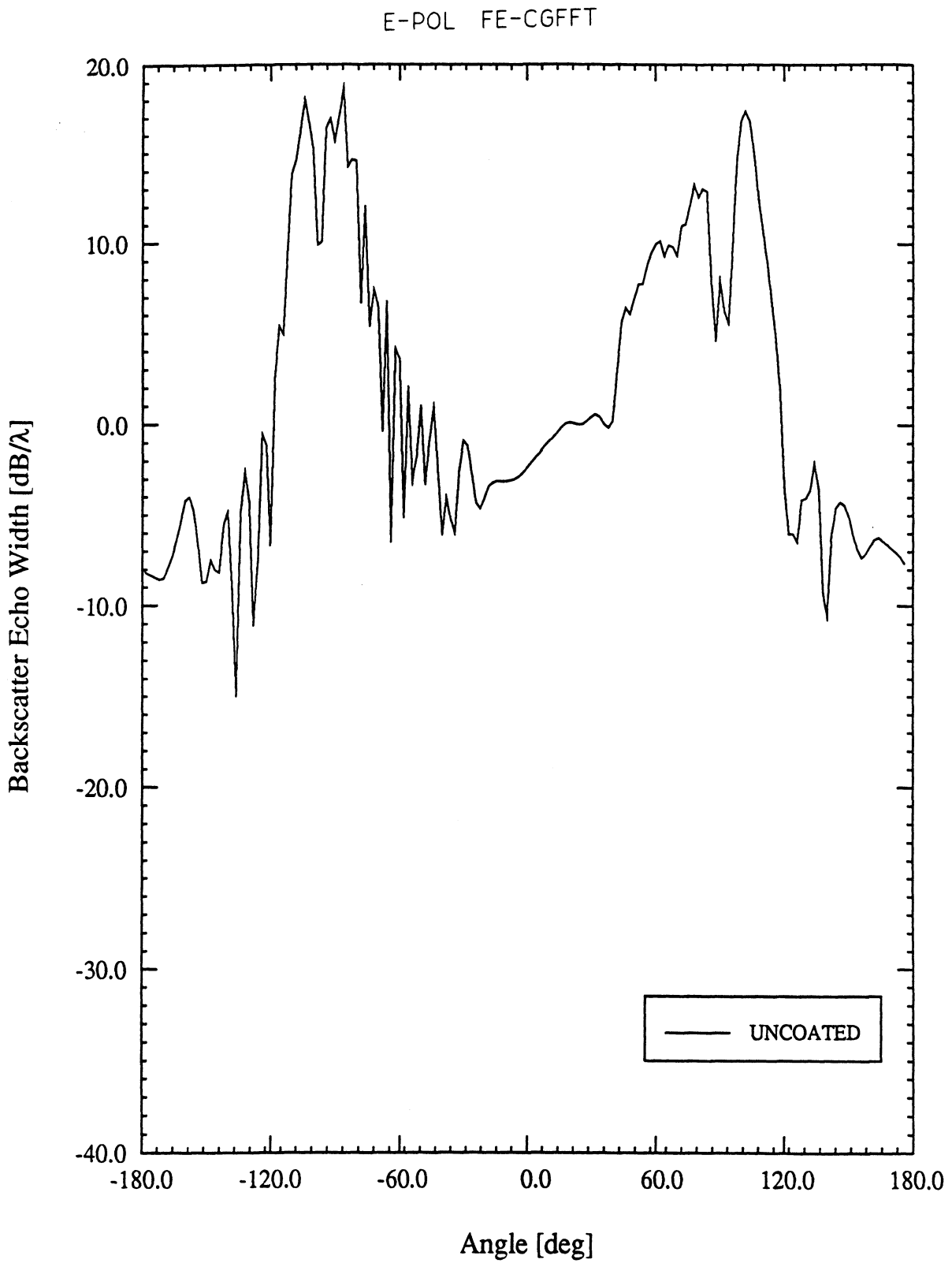


Figure 11: E-polarization echowidth for the airfoil given in figure 10.

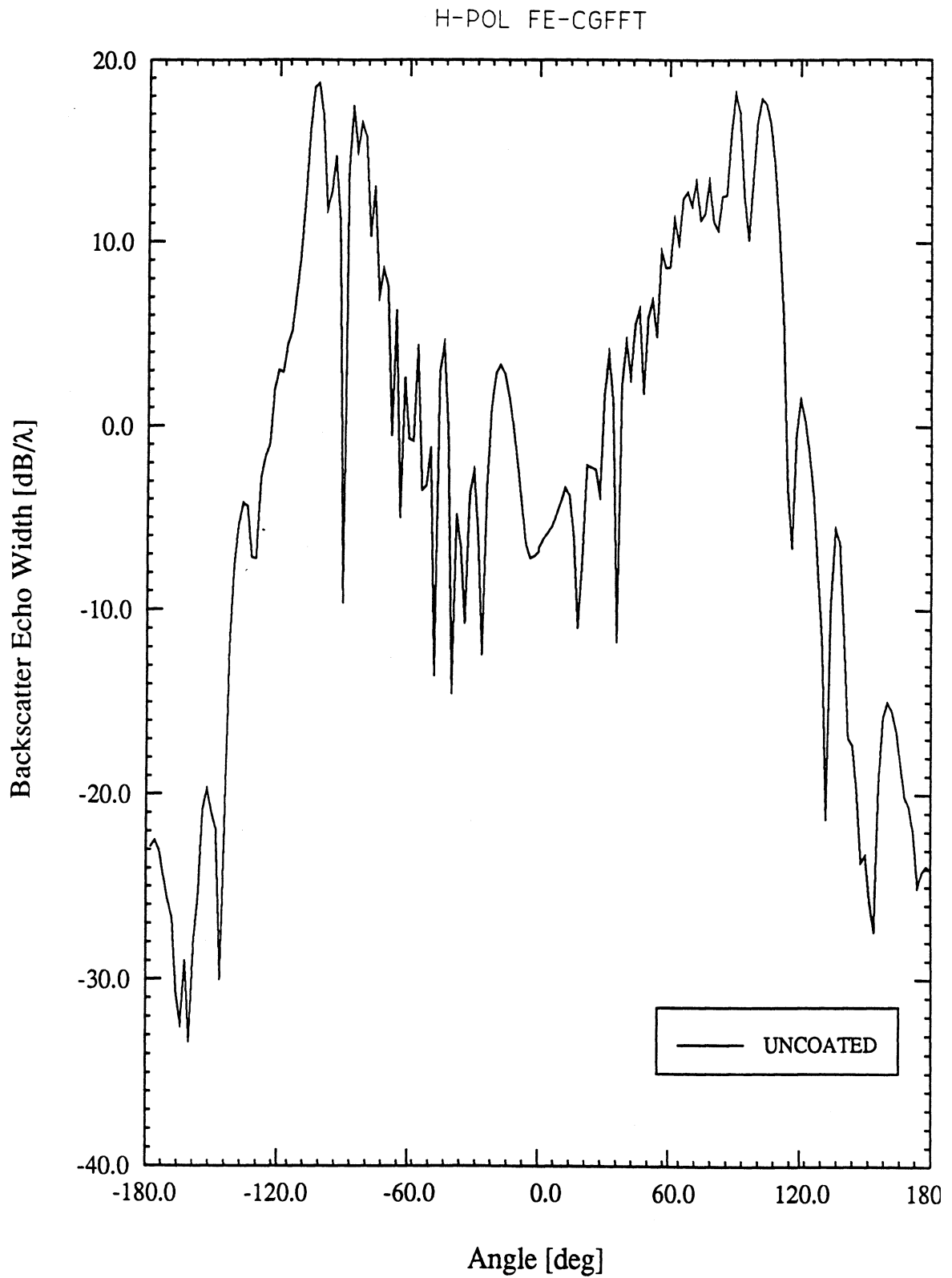


Figure 12: H-polarization echowidth for the airfoil given in figure 10.

Appendix A

Finite element formulation for tetrahedral elements and edge-based expansion basis

1 Derivation of finite element equations

Let us consider a three dimensional inhomogeneous body occupying the volume V . In order to discretize the electric field \mathbf{E} inside the body, we subdivide the volume V into a number of small tetrahedra, each occupying volume $V_e (e = 1, 2, \dots, M)$ with M being the total number of tetrahedral elements. Within each tetrahedron, the electric field satisfies the vector wave equation

$$\nabla \times \frac{1}{\mu_r} \nabla \times \mathbf{E} - k_o^2 \epsilon_r \mathbf{E} = 0 \quad (1)$$

where μ_r is the permeability of the medium, ϵ_r is the medium permittivity and k_o is the free space wave number. The next step is to expand the electric field within V_e as

$$\mathbf{E} = \sum_{j=1}^6 E_j^e \mathbf{W}_j^e \quad (2)$$

where \mathbf{W}_j^e are edge-based vector basis functions and E_j^e denote the expansion coefficients of the basis, all defined within the volume V_e . \mathbf{W}_j^e is tangential to the j th edge of the e th tetrahedron with zero tangential component along the other edges of the tetrahedral element. On substituting (2) into (1), we obtain

$$\sum_{j=1}^6 E_j^e \left(\nabla \times \frac{1}{\mu_r} \nabla \times \mathbf{W}_j^e - k_o^2 \epsilon_r \mathbf{W}_j^e \right) = 0 \quad (3)$$

In order to solve for the unknown expansion coefficients E_j^e , we take the dot product of (3) with \mathbf{W}_i^e and then integrate the resulting equation over the element volume V_e (Galerkin's technique). The wave equation thus reduces to

$$\sum_{j=1}^6 E_j^e \int_{V_e} \mathbf{W}_i^e \cdot \left(\nabla \times \frac{1}{\mu_r} \nabla \times \mathbf{W}_j^e - k_o^2 \epsilon_r \mathbf{W}_j^e \right) dv \neq 0 \quad (4)$$

The first term in the integral of the above expression can be simplified by using basic vector identities. Since

$$\mathbf{W}_i^e \cdot \left(\nabla \times \frac{1}{\mu_r} \nabla \times \mathbf{W}_j^e \right) = \nabla \cdot \left[\frac{1}{\mu_r} (\nabla \times \mathbf{W}_j^e) \times \mathbf{W}_i^e \right] + \frac{1}{\mu_r} (\nabla \times \mathbf{W}_i^e) \cdot (\nabla \times \mathbf{W}_j^e)$$

the divergence theorem can be readily applied to (4) resulting in the following expression:

$$0 = \sum_{j=1}^6 E_j^e \left\{ \int_{V_e} \left(\frac{1}{\mu_r} (\nabla \times \mathbf{W}_i^e) \cdot (\nabla \times \mathbf{W}_j^e) - k_o^2 \epsilon_r \mathbf{W}_i^e \cdot \mathbf{W}_j^e \right) dv + \oint_{S_e} \left(\frac{1}{\mu_r} (\nabla \times \mathbf{W}_j^e) \times \mathbf{W}_i^e \right) \cdot d\mathbf{S} \right\} \quad (5)$$

where S_e denotes the surface enclosing V_e . Using vector identities, (5) can be further simplified to yield the weak form of Maxwell's equation:

$$\sum_{j=1}^6 E_j^e \int_{V_e} \left(\frac{1}{\mu_r} (\nabla \times \mathbf{W}_i^e) \cdot (\nabla \times \mathbf{W}_j^e) - k_o^2 \epsilon_r \mathbf{W}_i^e \cdot \mathbf{W}_j^e \right) dv = j\omega\mu_o \oint_{S_e} \mathbf{W}_i^e \cdot (\mathbf{n} \times \mathbf{H}) ds \quad (6)$$

where $\mathbf{n} \times \mathbf{H}$ is the tangential magnetic field on the exterior dielectric surface. Equation (6) can be conveniently written in matrix form as

$$[A^e][E^e] = [B^e] \quad (7)$$

where

$$A_{ij}^e = \int_{V_e} \left(\frac{1}{\mu_r} (\nabla \times \mathbf{W}_i^e) \cdot (\nabla \times \mathbf{W}_j^e) - k_o^2 \epsilon_r \mathbf{W}_i^e \cdot \mathbf{W}_j^e \right) dv \quad (8)$$

$$B_i^e = j\omega\mu_o \oint_{S_e} \mathbf{W}_i^e \cdot (\mathbf{n} \times \mathbf{H}) ds \quad (9)$$

On assembling all the M tetrahedral elements that make up the geometry, we obtain a system of equations whose solution yields the field components over the entire body. Therefore, summing over all M elements, we have

$$\sum_{e=1}^M [A^e][E^e] = \sum_{e=1}^M [B^e] \quad (10)$$

which gives

$$[A][E] = [B] \quad (11)$$

where $[A]$ is a $N \times N$ matrix with N being the total number of edges resulting from the subdivision of the body and $[E]$ is a $N \times 1$ column vector denoting the edge fields. Due to the continuity of the tangential component of the magnetic field at the interface between two dielectrics, an element face lying inside the body does not contribute to $[B]$ since the surface integrals over the faces of adjacent tetrahedra cancel each other. As a result, $[B]$ is a column vector containing the tangential magnetic field only over the exterior surface of the body. Equation (11) can therefore be written as

$$\begin{aligned} A_{ss}\mathbf{E}_s + A_{si}\mathbf{E}_i &= \mathbf{H}_s \\ A_{is}\mathbf{E}_s + A_{ii}\mathbf{E}_i &= 0 \end{aligned} \quad (12)$$

where the subscript s denotes the edges on the surface and i represents the edges inside the body. It is thus readily seen that (11) relates the electric field inside and on the surface of the body to the on-surface tangential magnetic field.

2 Basis functions

Vector fields within tetrahedral domains in three dimensional space can be conveniently represented by expansion functions that are linear in the spatial variables and have either zero divergence or zero curl. The basis functions defined below are associated with the six edges of the tetrahedron and have zero divergence and constant curl. Assuming the four nodes and the six edges of a tetrahedron are numbered according to Table 1, the vector basis functions associated with the $(7 - i)$ th edge of the tetrahedron are defined as

$$\mathbf{W}_{7-i} = \begin{cases} \mathbf{f}_{7-i} + \mathbf{g}_{7-i} \times \mathbf{r}, & \mathbf{r} \text{ in the tetrahedron} \\ 0, & \text{otherwise} \end{cases} \quad (13)$$

where $i = 1, 2, \dots, 6$ and \mathbf{f} and \mathbf{g} are constant vectors. On direct evaluation, it is readily seen that

$$\nabla \cdot \mathbf{W}_i = 0 \quad (14)$$

$$\nabla \times \mathbf{W}_i = 2\mathbf{g}_i \quad (15)$$

Since the complex scalar E_j in (2) is the projection of the electric field onto the j th edge of the tetrahedral element,

$$\mathbf{W}_i \cdot \mathbf{e}_j |_{\mathbf{r} \text{ on } j\text{th edge}} = \delta_{ij} \quad (16)$$

where δ_{ij} is the Kronecker delta. Solving (13) and (16) for the unknown vectors yield[1]

$$\mathbf{f}_{7-i} = \frac{b_{7-i}}{6V} \mathbf{r}_{i_1} \times \mathbf{r}_{i_2} \quad (17)$$

$$\mathbf{g}_{7-i} = \frac{b_i b_{7-i} \mathbf{e}_i}{6V} \quad (18)$$

where V is the volume of the tetrahedral element, $\mathbf{e}_i = (\mathbf{r}_{i_2} - \mathbf{r}_{i_1})/b_i$ is the unit vector of the i th edge and $b_i = |\mathbf{r}_{i_2} - \mathbf{r}_{i_1}|$ is the length of the i th edge. All distances are measured with respect to the origin.

Since there are two numbering systems, local and global, a unique global direction is defined (e.g., always pointing from the smaller node number to the larger node number) to ensure the continuity of $\mathbf{n} \times \mathbf{E}$ across all edges. This implies that (13) should be multiplied by (-1) if the local edge vector (as defined in Table 1) does not have the same direction as the global edge direction. Even though \mathbf{W}_i forces no conditions on the normal component of \mathbf{E} , it has been shown[2] that the continuity of electric flux can be satisfied within the degree of approximation with the above formulation. Finally, since $\nabla \cdot \mathbf{W}_i = 0$ the electric field obtained through (2) exactly satisfies the divergence equation within the element, i.e. $\nabla \cdot \mathbf{E} = 0$. Therefore, the finite element solution is free from contamination of spurious solutions[2].

3 Mesh termination

Differential equation methods, such as finite elements, can only solve boundary value problems. Since electromagnetic problems are open boundary-infinite domain types, a means to truncate the solution domain to lie within a finite boundary must be found. On this boundary, a condition is enforced thus ensuring that the fields will obey the Sommerfeld

radiation condition at distances asymptotically far from the object. These absorbing boundary conditions (ABCs) have a significant advantage over the global methods of solving unbounded problems using finite elements in that they are local in nature. Due to this, the sparse matrix structure of the finite element formulation is retained. One disadvantage, however, is that ABCs are approximate and do not model the exterior field exactly. The objective of absorbing boundary conditions is to truncate the finite element mesh with boundary conditions that cause minimum reflections of an outgoing wave. These ABCs should provide small, acceptable errors while minimising the distance from the object of interest to the outer boundary. This minimal distance is required to reduce the number of unknowns in the problem for computational efficiency. A three dimensional vector boundary condition will be investigated here for terminating the finite element mesh of the body described in section 1.1. We begin with the Wilcox representation[3] of the electric field which has an expansion

$$\mathbf{E}(\mathbf{r}) = \frac{e^{-jkr}}{r} \sum_{n=0}^{\infty} \frac{\mathbf{A}_n(\theta, \phi)}{r^n} \quad (19)$$

From (19), we get

$$\nabla \times \mathbf{E} = \left\{ jk\hat{r} \times \frac{1 + D_1}{r} \right\} \mathbf{E} - \frac{e^{-jkr}}{r^2} \sum_{n=1}^{\infty} \frac{n\mathbf{A}_{nt}}{r^n} \quad (20)$$

where $\mathbf{A}_{nt} = \hat{r} \times \mathbf{A}_n$ is the transverse component of \mathbf{A}_n and, for a vector \mathbf{F} , $D_1\mathbf{F}$ is given by

$$\begin{aligned} D_1\mathbf{F} = & \frac{1}{\sin\theta} \left[\frac{\partial}{\partial\theta}(\sin\theta F^\phi) - \frac{\partial F^\theta}{\partial\phi} \right] \hat{r} \\ & + \frac{1}{\sin\theta} \left[\frac{\partial F^r}{\partial\theta} - \sin\theta F^\phi \right] \hat{\theta} + \left[F^\theta - \frac{\partial F^r}{\partial\theta} \right] \hat{\phi} \end{aligned} \quad (21)$$

Using the recursion relation

$$-2jkn\mathbf{A}_{nt} = n(n-1)\mathbf{A}_{n-1,t} + D_4\mathbf{A}_{n-1}$$

where

$$\begin{aligned}
D_4 \mathbf{A}_n &= (D A_n^\theta + D_\theta \mathbf{A}_n) \hat{\theta} + (D A_n^\phi + D_\phi \mathbf{A}_n) \hat{\phi} \\
D_\theta \mathbf{A}_n &= 2 \frac{\partial A_n^r}{\partial \theta} - \frac{1}{\sin^2 \theta} A_n^\theta - \frac{2 \cos \theta}{\sin^2 \theta} \frac{\partial A_n^\phi}{\partial \theta} \\
D_\phi \mathbf{A}_n &= \frac{2}{\sin \theta} \frac{\partial A_n^r}{\partial \phi} - \frac{1}{\sin^2 \theta} A_n^\phi + \frac{2 \cos \theta}{\sin^2 \theta} \frac{\partial A_n^\theta}{\partial \phi}
\end{aligned}$$

and D is Beltrami's operator[3], we can derive the representation correct to r^{-4} . Applying the recursion relation in (20) yields the desired relationship for the vector ABC:

$$\nabla \times \mathbf{E} = \alpha(r) \mathbf{E} + \beta(r) D_4 \mathbf{E} \quad (22)$$

where

$$\alpha(r) = jk \left\{ \frac{D_1}{jkr} - \left(1 + \frac{1}{jkr} \right) \hat{r} \times \right\} \quad (23)$$

$$\beta(r) = \frac{1}{2jkr^2} \frac{1}{(1 + 1/jkr)} \quad (24)$$

The ABC formulated above is applicable to spherical boundaries and hence would be storage intensive and numerically inefficient when used to terminate the mesh of long and thin geometries. It would be highly desirable to choose an outer boundary that conforms to the shape of the object. An approximate boundary condition based on the asymptotic representation of fields for a two dimensional scalar problem has already been derived[4]. It is the author's intention to extend the derivation of the two dimensional scalar boundary condition to a three dimensional vector absorbing boundary condition for an arbitrary outer boundary.

4 Solution of the finite element equations

An inspection of (11) reveals that for an inhomogeneous body, there is no a priori information about the tangential magnetic field over the exterior surface of the body. Relation (11) therefore contains two unknown vectors, $[E]$ and $[B]$, and thus another condition is required involving the two variables to permit an evaluation of the fields inside and on the surface of the body. This condition relating the tangential electric field to the tangential magnetic field on the surface is provided by (22). Since the ABC in (22) refers to the scattered field, we can rewrite it as

$$\begin{aligned}
\nabla \times \mathbf{E}_s^s &= \alpha(r)\mathbf{E}_s^s + \beta(r)D_4\mathbf{E}_s^s \\
\mathbf{H}_s^s &= \frac{j}{\omega\mu} [\alpha(r)\mathbf{E}_s^s + \beta(r)D_4\mathbf{E}_s^s] \\
&= \mathcal{K}\mathbf{E}_s^s
\end{aligned} \tag{25}$$

where $\mathcal{K} = \frac{j}{\omega\mu} [\alpha(r) + \beta(r)D_4]$ and the subscript s denotes the field on the surface and the superscript s represents the scattered field. Since the total field is a sum of the incident field and the scattered field, therefore from (25), we obtain

$$\begin{aligned}
\mathbf{H}_s^s &= \mathcal{K}\mathbf{E}_s^s \\
\mathbf{H}_s - \mathbf{H}_s^{inc} &= \mathcal{K}(\mathbf{E}_s - \mathbf{E}_s^{inc})
\end{aligned} \tag{26}$$

Substituting (26) into (12) and simplifying gives

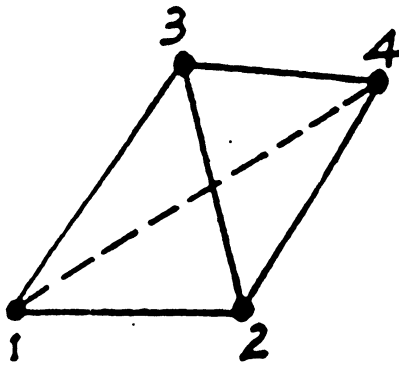
$$\begin{aligned}
(A_{ss} - \mathcal{K})\mathbf{E}_s + A_{si}\mathbf{E}_i &= \mathbf{H}_s^{inc} - \mathcal{K}\mathbf{E}_s^{inc} \\
A_{is}\mathbf{E}_s + A_{ii}\mathbf{E}_i &= 0
\end{aligned} \tag{27}$$

The above equation can thus be solved for the unknown electric fields both inside and on the surface of the body.

5 References for Appendix A

1. M.L. Barton and Z.J. Cendes, "New vector finite elements for three-dimensional magnetic field computation", *J. Appl. Phys.*, vol.61, no.8, pp.3919-21, April 1987.
2. X. Yuan, "On the use of divergenceless basis functions in finite elements", submitted to *Electron. Lett.*
3. C.H. Wilcox, "An expansion theorem for electromagnetic fields", *Comm. Pure Appl. Math.*, vol. 9, pp. 115-134, May 1956.
4. A. Khebir, O.M. Ramahi and R. Mittra, "An efficient partial differential equation method to solve complex shape scatterers", to appear.

TABLE I
TETRAHEDRON EDGE DEFINITION



Edge #	i_1	i_2
1	1	2
2	1	3
3	1	4
4	2	3
5	4	2
6	3	4

Task Title **Analytical Solutions with
Generalized Impedance
Boundary Conditions**

Investigators **H.H. Syed and J.L. Volakis**

Period Covered **Sept. 1990 - Feb. 1991**

ABSTRACT

Rigorous UTD (uniform Geometrical Theory of Diffraction) diffraction coefficients are presented for a coated convex cylinder simulated with generalized impedance boundary conditions. In particular, ray solutions are obtained which remain valid in the transition region and reduce uniformly to those in the deep lit and shadow regions. These involve new transition functions in place of the usual Fock-type integrals, characteristic to the impedance cylinder. A uniform asymptotic solution is also presented for observations in the close vicinity of the cylinder. As usual, the diffraction coefficients for the convex cylinder are obtained via a generalization of the corresponding ones for the circular cylinder.

OBJECTIVE

This task involves the use of higher order boundary conditions to generate new solutions in diffraction theory. In particular, diffraction coefficients will be developed for dielectric/magnetic layers and metal-dielectric junctions which are often encountered on airborne vehicles as terminations of coatings and conformal antennas. Solutions for both polarizations will be developed for fairly thick junctions and versatile computer codes will be written and tested. Creeping wave diffraction coefficients will be also developed for multilayered coated cylinders.

PROGRESS

1. Introduction

The problem of scattering by a smooth convex impedance cylinder has received much attention. Wang [1, 2] presented ray-optical solutions for the impedance and coated cylinders. His results are valid only in the deep lit and shadow regions and do not apply to the case where the observation point is in the transition region. Wait and Conda [3, 4] developed a solution which is valid in the transition region and for observation points on and off the surface. However, as pointed out by Pathak [5] it did not uniformly reduce to the ray solution [6, 7] exterior to the transition regions. Also, it is not valid on the portion of the surface in the transition region and these limitations were the primary motivation in Pathak's work [5] for the perfectly conducting convex cylinder. Recently, Kim and Wang [8] presented a solution applicable to a coated cylinder that remained valid in the transition region. They employed a heuristic approach to obtain the numerical values of the resulting transition integral applicable to a coated cylinder. Their solution is uniform but is not applicable to the close vicinity of the cylinder.

Here we develop a rigorous UTD solution of the diffraction by a coated cylinder simulated with generalized impedance boundary conditions. In addition, a uniform asymptotic solution is obtained which remains valid when the observation point is in close vicinity of the cylinder. An important aspect of the paper is also the use of second order generalized impedance boundary conditions (GIBC) for the simulation of the coating. Their derivation has already been given in [9] and [10] and are characterized by the inclusion of higher order field derivatives in their definition. Because of this they are less local which leads to an improved simulation (with respect to the standard impedance boundary condition - SIBC) of the coating in a manner analogous to the order of the highest derivative kept in the condition. Recently, they were successfully applied to a number of diffraction problems [11], [12] and have also been used in numerical simulations of multilayer coatings (see fig. 1) [13]. These applications provided a measure of the accuracy of the proposed GIBC and in particular accuracy criteria were derived in [13] for the second order conditions as a function of coating thickness and composition.

The UTD solution to be presented here parallels that given by Pathak [5] for the circular perfectly conducting cylinder. However, in the case of the coated cylinder the resulting UTD expressions are in terms of Fock-type integrals whose efficient evaluation is of primary interest. In the following we first present the eigenfunction solution based on

the second order GIBC simulation of a circular coated cylinder. By employing Watson's transformation this is written in integral form which is then cast in a ray representation. The ray solution is subsequently generalized to the case of a general convex cylinder. Finally, the evaluation of the Fock-type integrals is discussed and some results are presented which validate the accuracy of the GIBC eigenfunction and ray solutions. In the process, we demonstrate the improved accuracy of the GIBC solution over the corresponding SIBC solution, and it is also shown how the presented UTD solution can be extended to treat multilayered coated cylinders.

The details of the analysis are described in the report 025921-13-T which was recently submitted to the sponsor. Below we only attach a few results which demonstrate the accuracy and utility of the derived formulae.

2. Numerical Results

The UTD expressions derived in the UM report 025921-17-T provide a complete set of equations for the computation of the total field in all regions of interest. Below, we present some calculated data which validate the accuracy of the derived expressions by comparison with data based on the moment method and eigenfunction solutions.

In figure 2 the eigenfunction solutions based on the GIBC and SIBC simulations are compared with the exact for a coated cylinder and this clearly demonstrates the improved simulation (with respect to the standard impedance boundary conditions - SIBC) achieved with the second order GIBC. To show the validity of the UTD solution in the case of the convex cylinder, a special case of an elliptical cylinder is considered in figure 3. Data based on the moment method are compared with those obtained from the UTD solution in conjunction with the second order low and high contrast boundary conditions.

Figure 4 verifies the asymptotic solution developed for the field point in the close vicinity of a convex cylinder. We remark, however, that the approximations used for the Hankel functions in the derivation of (42) and (43) become less accurate for some values of ϵ_r and μ_r associated with lossless coatings, and this can be avoided by using more accurate approximations for the Hankel functions. Finally, figure 5 demonstrates the use of GIBC in simulating multilayer coatings by simply redefining the material constants a_m and a_m' as discussed in [10, 13].

A difficulty in implementing the expressions derived in this paper was the evaluation of the Fock-type integrals $G(x,q)$, $g_1(D)$ and $g_2(D)$ as well as determination of the zeros corresponding to (21). The Fock-type integrals were evaluated by employing the

method described in [16] and the zeros of (21) were determined using the routine given in [20].

Summary

Rigorous ray solutions of the scattered fields were presented for a coated convex cylinder. These were developed in the context of the uniform geometrical theory of diffraction and specific expressions were given for the scattered fields in the lit, shadow and transition regions as well as for observations in the near vicinity of the cylinder. That is, UTD expressions were derived for all regions exterior to the coated cylinder. These are suited for engineering computations and are given in terms of the generalized Pekeris or Fock-type functions whose evaluation was efficiently performed via the Fourier Trapezoidal rule suggested by Pearson [16].

In comparison to the solution given by Kim and Wang [8], the ray representations given here are based on a second order generalized impedance boundary condition which permits the simulation of thin multilayered coating as demonstrated in the included examples. Also, in our implementation of the transition fields we employed a rigorous rather than a heuristic evaluation of the Fock-type integrals. Further, we have presented accurate field representations for observations on or near the vicinity of the coated cylinder and these can also be used for computing the radiated fields by a source or an aperture on the surface of the convex cylinder.

REFERENCES

- [1] N. Wang, "Regge poles, natural frequencies, and surface wave resonance of a circular cylinder with a constant surface impedance," *IEEE Trans. Antenna & Propagat.*, Vol. AP-30, Nov. 1982.
- [2] ----, "Electromagnetic scattering from a dielectric coated circular cylinder," *IEEE Trans. Antenna & Propagat.*, Vol. AP-33, Sept. 1985.
- [3] J.R. Wait and A.M. Conda, "Diffraction of electromagnetic waves by smooth obstacles for grazing angles," *J. Res. Bur. Stand.*, Vol. 63D, pp. 181-197, 1959.
- [4] ----, "Pattern of an antenna on a curved lossy surface," *IRE Trans. Antennas & Propagat.*, Vol. AP-6, pp. 348-359, Oct. 1958.

- [5] P.H. Pathak, "An asymptotic analysis of the scattering of plane waves by a smooth convex cylinder," *Radio Sci.*, Vol. 14, pp. 419-435, 1979.
- [6] J.B. Keller, "Diffraction by a convex cylinder," *IEEE Trans. Antenna & Propagat.*, Vol. AP-24, pp. 312-321, 1956.
- [7] ----, "Geometrical theory of diffraction," *J. Opt. Soc. Amer.*, Vol. 52, pp. 116-130, 1962.
- [8] H. Kim and N. Wang, "UTD solution for electromagnetic scattering by a circular cylinder with thin lossy coatings," *IEEE Trans. Antenna & Propagat.*, Vol. AP-37, pp. 1463-1472, Nov. 1989.
- [9] T.B.A. Senior and J.L. Volakis, "Derivation and application of a class of generalized boundary conditions," *IEEE Trans. Antenna & Propagat.*, Vol. AP-37, pp. 1566-1572, Dec. 1989.
- [10] M.A. Ricoy and J.L. Volakis, "Derivation of generalized transition/boundary conditions for planar multiple layer structures," *Radio Sci.*, Vol. 25, pp. 391-405, July - August 1990.
- [11] ----, "Diffraction by a symmetric material junction, Part I: general solution," submitted to *IEEE Trans. Antenna & Propagat.*
- [12] ----, "Diffraction by a symmetric material junction, Part II: boundary conditions," submitted to *IEEE Trans. Antenna & Propagat.*
- [13] J.L. Volakis and H.H. Syed, "Application of higher order boundary conditions to scattering by multilayered coated cylinders," *J. of Electromagnetic Waves and Applications*. (in press)
- [14] J.J. Bowman, T.B.A. senior and P.L.E. Uslenghi, "Electromagnetic and Acoustic Scattering by Simple Shapes," Amsterdam: North-Holland, 1969.
- [15] N.A. Logan and K.S. Yee, "Electromagnetic Waves," edited by R.E.Langer, University of Wisconsin Press, Madison.

- [16] L.W. Pearson, "A scheme for automatic computation of Fock-type integrals," *IEEE Trans. Antenna & Propagat.*, Vol. AP-35, pp. 1111-1118, Oct. 1987.
- [17] O.A. Tuck, "A simple 'Finlon-trapezoid' rule," *Math. Comp.*, Vol. 21, pp. 239-241, 1967.
- [18] L. Felson and N. Marcuvitz, "Radiation and Scattering of Waves," Prentice Hall, 1973.
- [19] R.G. Kouyoumjian and P.H. Pathak, "A uniform geometrical theory of diffraction for an edge in a perfectly conducting surface," *Proc. IEEE*, Vol. 62, pp. 1448-1461, 1974.
- [20] B.K. Singaraju, D.V. Giri and C.E. Baum, "Further development in the application of contour integration to the evaluation of the zero of analytical functions and relevent computer programs," *Math. Note* 24, March 1976.

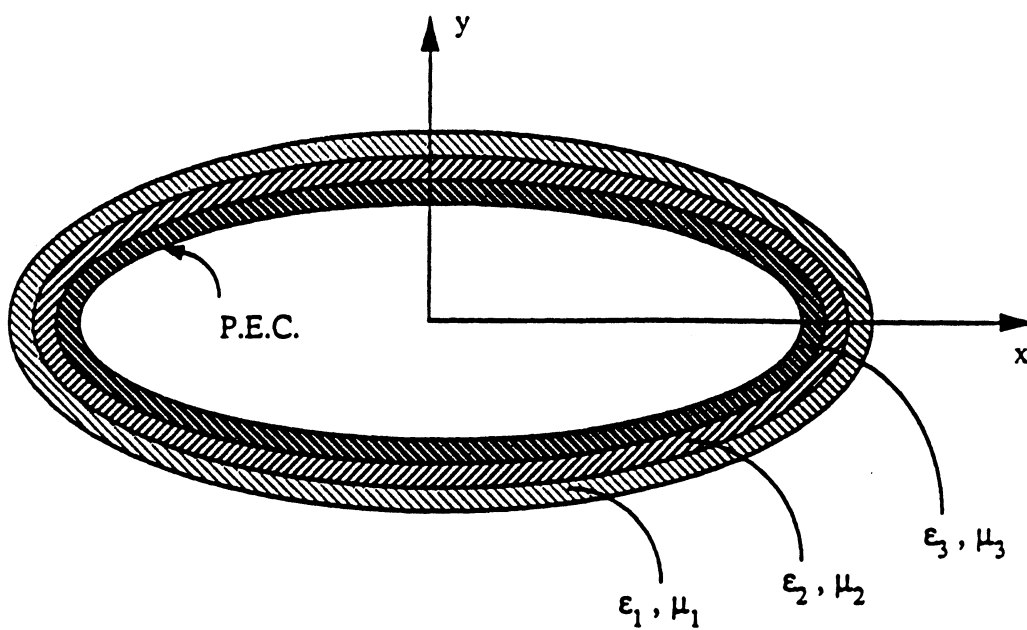
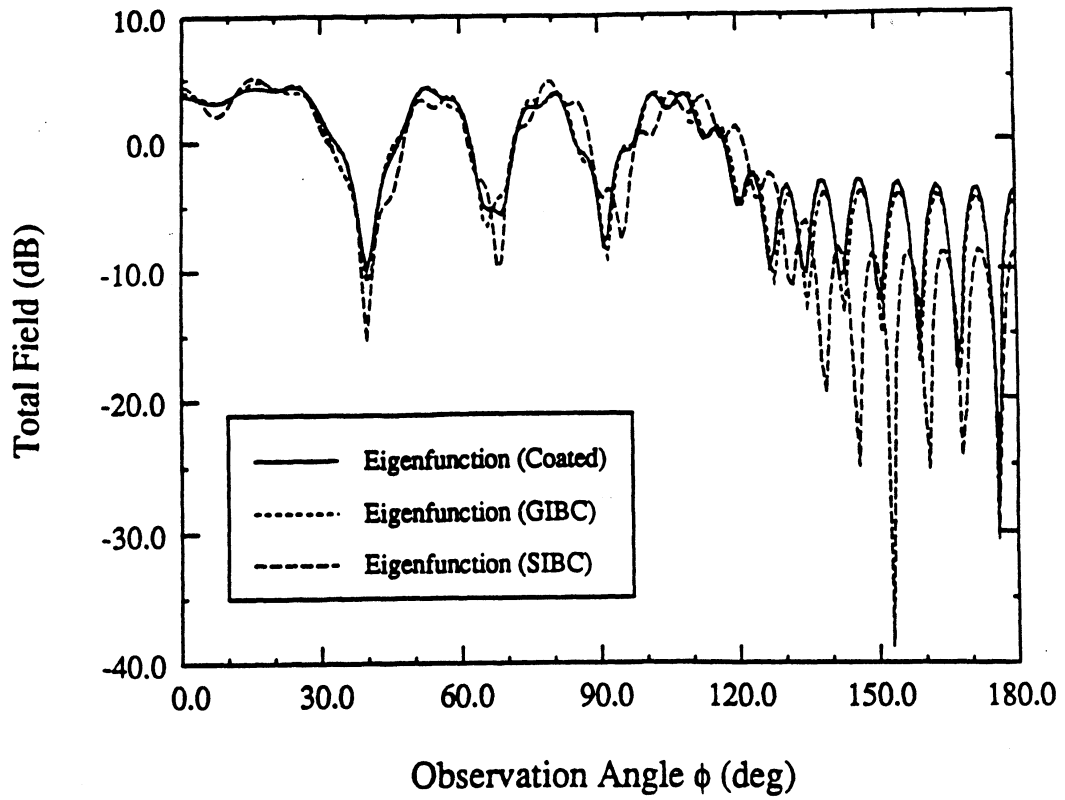
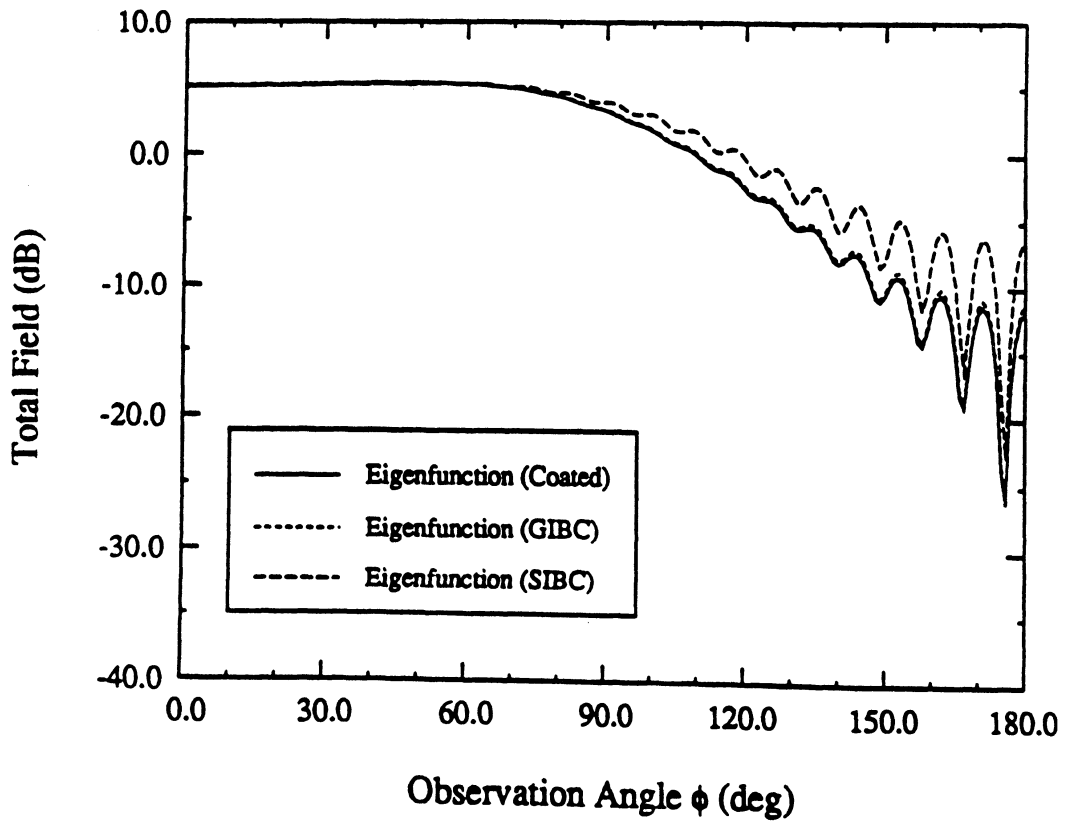


Fig. 1. Illustration of a three-layer coated cylinder.



(a)



(b)

Fig. 2: Bistatic H-polarization scattering pattern for a circular cylinder having $b = 3\lambda$, (a) $\epsilon_r = 4$, $\mu_r = 1$, $\delta = 0.07\lambda$, $\rho = 5\lambda$ (b) $\epsilon_r = 8$, $\mu_r = 1$, $\delta = 0.2\lambda$, $\rho = 3.05\lambda$.

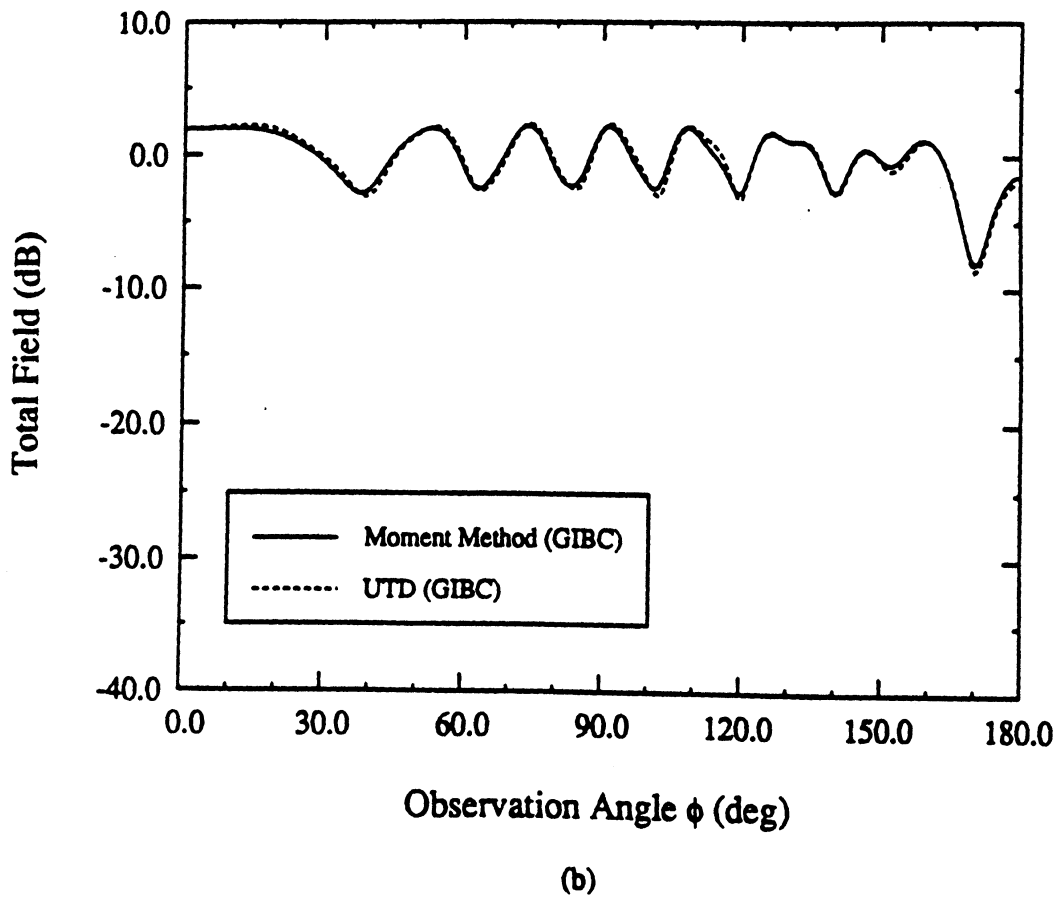
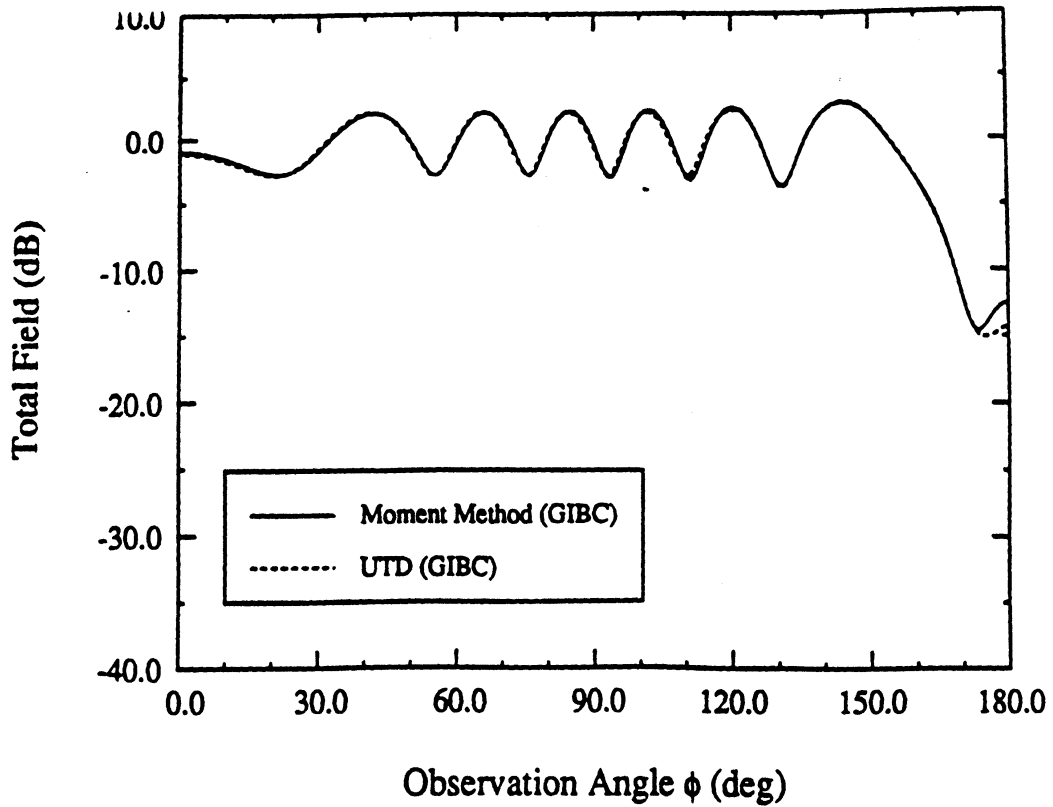
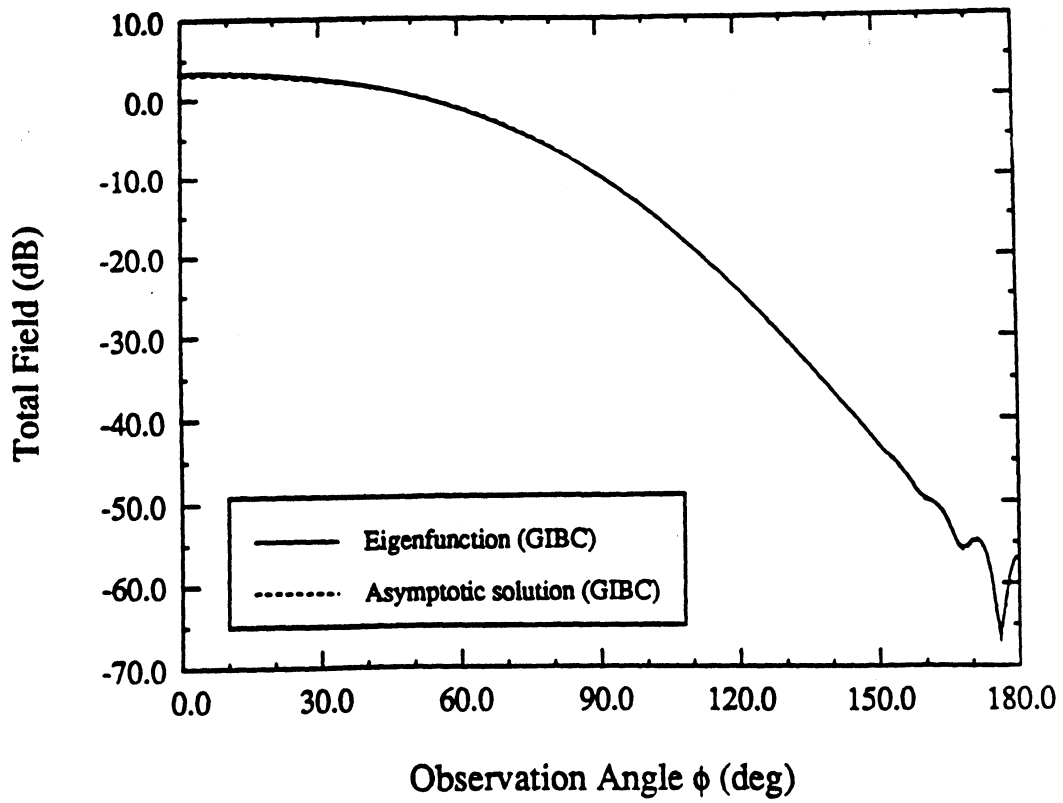
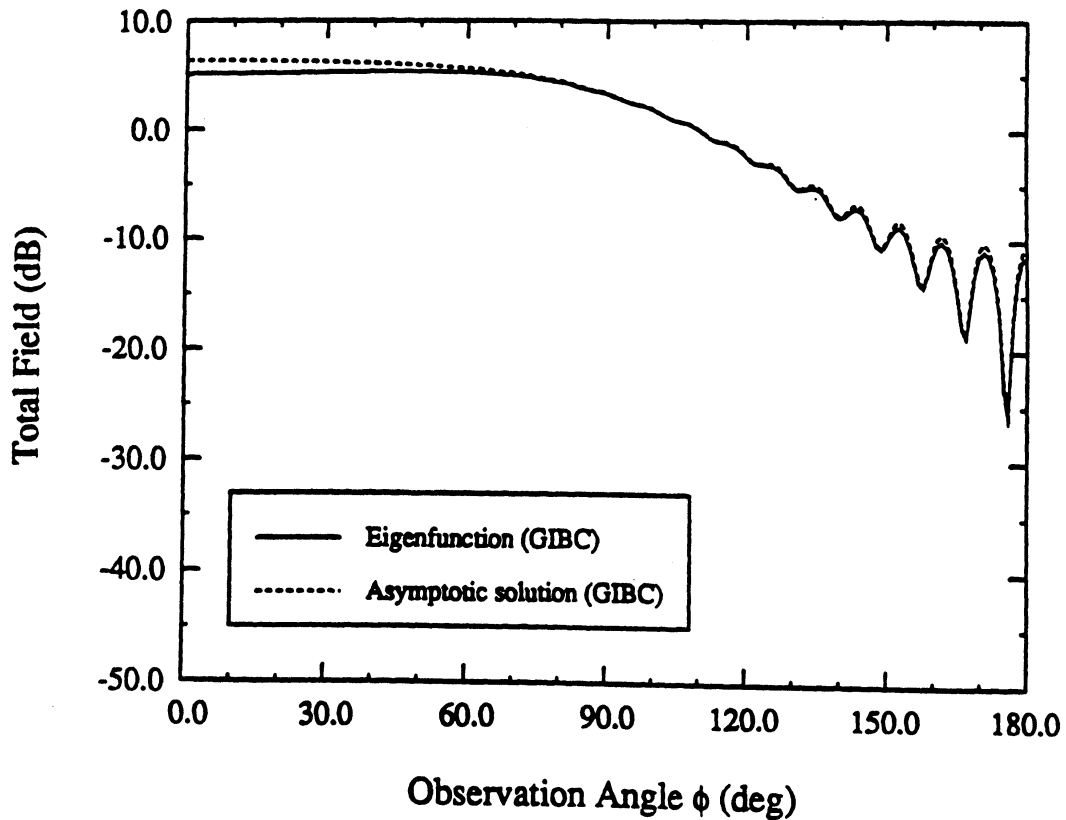


Fig. 3: Bistatic scattering pattern for an elliptical cylinder having $a = 2\lambda$, $b = 1\lambda$, $\rho = 5\lambda$, $\phi_i = 0$ (a) E-polarization, $\epsilon_r = 4$, $\mu_r = 1$, $\delta = 0.07\lambda$ (b) H-polarization, $\epsilon_r = 8$, $\mu_r = 1$, $\delta = 0.2\lambda$.

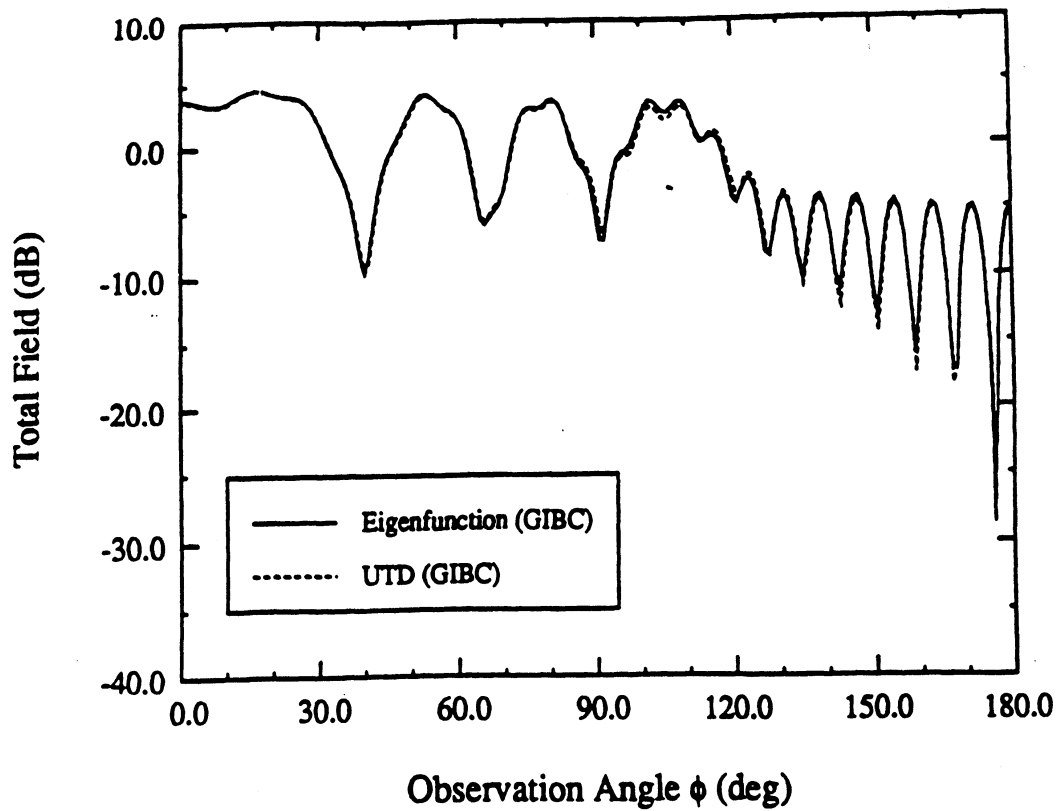


(a)

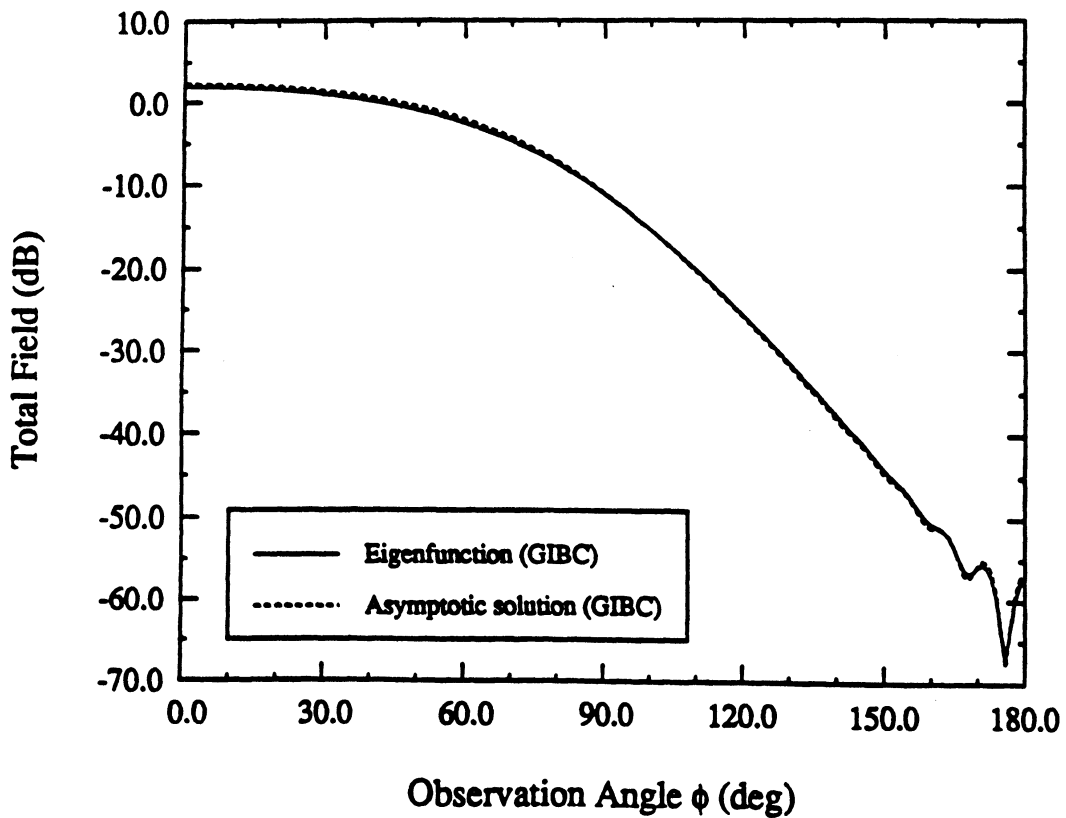


(b)

Fig. 4: Bistatic scattering pattern of a circular cylinder having $b = 3\lambda$, $\rho = 3.05\lambda$, $\phi_i = 0$ (a) E-polarization, $\epsilon_r = 4$, $\mu_r = 1$, $\delta = 0.07\lambda$ (b) H-polarization, $\epsilon_r = 8$, $\mu_r = 1$, $\delta = 0.2\lambda$.



(a)



(b)

Fig. 5: Bistatic scattering pattern of a three-layer coated circular cylinder having $b = 3\lambda$, $\phi_i = 0$, $\epsilon_{r1} = 3 - j0.1$, $\epsilon_{r2} = 4 - j0.3$, $\epsilon_{r3} = 7 - j1.5$, $\mu_{r1} = \mu_{r2} = \mu_{r3} = 1$, $\delta_1 = 0.01\lambda$, $\delta_2 = 0.02\lambda$, $\delta_3 = 0.03\lambda$ (a) H-polarization, $\rho = 5\lambda$ (b) E-polarization, $\rho = 3.05\lambda$.

PAPER WRITTEN (TO DATE) UNDER THIS GRANT

1. J.-M. Jin and J.L. Volakis, "A New Technique for Characterizing Diffraction by Inhomogeneously Filled Slot of Arbitrary Cross Section in a Thick Conducting Plane," *IEE Electronic Letters*, Vol. 25, No. 17, pp. 1121-1122, 17th Aug. 1989.
2. J.-M. Jin, J.L. Volakis and V.V. Liepa, "A Moment Method Solution of Volume-Surface Integral Equation Using Isoparametric Elements and Point-Matching," *IEEE Trans. Microwave Theory and Techniques*, vol. MTT-37, pp. 1641-1645, Oct. 1989.
3. J.L. Volakis and M.A. Ricoy, "H-polarization Diffraction by a Thick Metal-Dielectric Join," *IEEE Trans on Antennas and Propagat.*, Vol. AP-37, pp. 1453-1462, Nov. 1989.
4. T.B.A. Senior and J.L. Volakis, "Derivation and Application of a Class of Generalized Boundary Conditions," *IEEE Trans. on Antennas and Propagat.*, Vol. AP-37, PP. 1566-1572, Dec. 1989.
5. K. Barkeshli and J.L. Volakis, "On the Implementation and Accuracy of the Conjugate Gradient Fourier Transform Method," *IEEE Transactions Antennas and Propagation Magazine*, Vol. 32, No.2, pp. 20-26, April 1990.
6. J.-M. Jin and J.L. Volakis, "TM Scattering by an Inhomogeneously Filled Aperture in a Thick Ground Plane," *IEE Proceedings, Part H*. Vol. 137, No. 3, pp. 153-159, June 1990.
7. J.-M. Jin and J.L. Volakis, "TE Scattering by an Inhomogeneously Filled Aperture in a Thick Conducting Plane," *IEEE Trans. Antennas and Propagat.*, Vol AP-38, pp. 1280-1286, August 1990.
8. K. Barkeshli and J.L. Volakis, "TE Scattering by a Two-Dimensional Groove in a Ground Plane Using Higher Order Boundary Conditions," *IEEE Trans. Antennas and Propagat.*, pp.1421-1428, October 1990.
9. M.A. Ricoy and J.L. Volakis, "Derivation of Generalized Transition/Boundary Conditions for Planar Multiple Layer Structures," *Radio Sci.*, Vol. 25, pp. 391-405, July-Aug. 1990.
10. J.D. Collins and J.L. Volakis and J.M. Jin, "A Finite Element-Boundary Integral Formulation for Solution via CGFFT of Two-Dimensional Scattering Problems," *IEEE Trans. Antennas and Propagat.*, Vol. AP-38, pp. 1852-1858, November 1990.
11. J.L. Volakis and H.H. Syed, "Application of Higher Order Boundary Conditions to Scattering by Multi-layer Coated Cylinders," *J. of Electromagnetic Waves and Applications.*, Vol. 4, No. 12, pp. 1157-1180, 1990
12. J. D. Collins, J.-M. Jin and J.L. Volakis, "A Combined Finite Element-Boundary Element Formulation for Solution of Two-Dimensional Problems via CGFFT," *Electromagnetics*, Vol 10, pp. 423-437, 1990.

13. J.M. Jin and J.L. Volakis, " A Finite Element-Boundary Integral Formulation for Scattering by Three-Dimensional Cavity-Backed Apertures," *IEEE Trans. Antennas and Propagation.*, Vol. AP-39, pp. January 1991.
14. M.A. Ricoy and J. L. Volakis, "Diffraction by a Multilayered Slab Recessed in a Ground Plane via a Generalized Impedance Boundary Condition," *Radio Science*, March-April, 1991.
15. J.M. Jin and J.L. Volakis, "Electromagnetic Scattering by and Transmission through a Three-Dimensional Slot in a Thick Conducting Plane," *IEEE Trans. Antennas and Propagat...*, Vol. AP-39, April 1991
16. H.H. Syed and J.L. Volakis, "An Approximate Diffraction Coefficient for an Impedance Wedge at Skew Incidence," submitted to *IEEE Trans. Antennas and Propagat.*
17. J.M. Jin, J.L. Volakis and J.D. Collins, "A Finite Element-Boundary Element Method for Scattering by Two and Three Dimensional Structures," submitted to *IEEE Antennas and Propagat. Magazine.*
18. T.B.A. Senior and J.L. Volakis "Generalized Impedance Boundary Conditions in Scattering," accepted in *Proceedings of the IEEE.*
19. J.-M. Jin and J.L. Volakis, "A Unified Approach to Integral Equation Formulations for Electromagnetic Scattering," tutorial paper submitted to *IEEE Trans. Antennas and Propagat.*
20. M.A. Ricoy and J.L. Volakis, "Diffraction by a Symmetric Material Junction, Part I: General Solution," submitted to *IEEE Trans. Antennas and Propagat.*
21. M.A. Ricoy and J.L. Volakis, "Diffraction by a Symmetric Material Junction, Part II: Resolution of Non-Uniqueness Associated with Higher Order Boundary Conditions," submitted to *IEEE Trans. Antennas and Propagat.*
22. H.H. Syed and J.L. Volakis, "High Frequency Scattering by a Smooth Coated Cylinder Simulated with Generalized Impedance Boundary Conditions," submitted to *Radio Science*
23. J.M. Jin and J.L. Volakis, "Scattering by a Finite Frequency Selective Surface," submitted to the *IEEE Trans. Antennas and Propagat*

CONFERENCE PAPERS PRESENTED/WRITTEN TO DATE

1. J.D. Collins and J.L. Volakis, "A Boundary Integral Conjugate Gradient Fast Fourier Transform Method for Solving Two Dimensional Scattering Problems," 1989 IEEE URSI/AP-S symposium, Session 50, San Jose, CA. URSI Digest p. 216.
2. H.H. Syed and J.L. Volakis, "An Approximate Diffraction Coefficient for an Impedance Wedge at Skew Incidence," 1989 IEEE AP-S/URSI symposium, Session 57, San Jose, CA. AP-S Digest pp. 1286-1289.
3. M.A. Ricoy and J.L. Volakis, "Application of Higher Order Boundary Conditions in Scattering by Material Discontinuities," 1989 IEEE AP-S/URSI symposium, Session 63, San Jose, CA. URSI Digest p. 279.
4. J.L. Volakis (invited), "Application of CG and FFT to Simulations with Higher Order Boundary Conditions," 1989 IEEE AP-S/URSI symposium, San Jose, CA.
5. J.-M. Jin, V.V. Liepa and J.L. Volakis, "Applications of Isoparametric elements in the Numerical Solution of Electromagnetic Field Problems," ISAE 1989, China.
6. J.L. Volakis, "Numerical Implementation of Generalized Impedance Boundary Conditions," 1989 URSI Electromagnetic Theory Symposium, Aug. 1989, Stockholm, Sweden. Symposium Digest pp. 434-437.
7. K. Barkeshli and J.L. Volakis, "TE Scattering by a Two-Dimensional Groove in a Ground Plane Using Higher Order Boundary Conditions," 1990 IEEE AP-S/URSI Symposium, Dallas, Tx., URSI Digest p. 43.
8. M.A. Ricoy and J.L. Volakis, "Application of Generalized Impedance Boundary Conditions to Diffraction by a Multilayered Metal-Dielectric Junction," 1990 IEEE AP-S/URSI Symposium, Dallas, Tx., URSI Digest, p.62.
9. H.H. Syed and J.L. Volakis, "Diffraction by a Smooth Coated Cylinder simulated with Generalized Impedance Boundary Conditions," 1990 IEEE AP-S/URSI Symposium, Dallas, Tx., URSI Digest p. 176.
10. J.M. Jin and J.L. Volakis, "A FEM/BEM Formulation for a CG-FFT Solution of 2-D Scattering by Grooves and Thick Slots," 1990 IEEE AP-S/URSI Symposium, Dallas, Tx., URSI Digest p. 260.
11. J.D. Collins and J.L. Volakis, "A Combined Boundary Integral Finite Element Formulation for Solution of Three Dimensional Scattering via Conjugate Gradient Fast Fourier Transform Method," 1990 IEEE AP-S/URSI Symposium, Dallas, Tx., URSI Digest p. 263.
12. J.L. Volakis and H.H. Syed, "Application of Higher Order Boundary Conditions to Scattering by Multilayered Coated Cylinders," 1990 IEEE AP-S/URSI Symposium, Dallas, Tx., AP-S Digest pp. 586-589.

13. J. M. Jin and J.L. Volakis, "A FEM/BEM Formulation for a CG-FFT Solution of 3-D Scattering by a Cavity," 1990 IEEE AP-S/URSI Symposium, Dallas, Tx., AP-S Digest pp. 1726-1729.
14. J.M. Jin, J.L. Volakis and J.D. Collins, "A Finite Element Boundary Integral Formulation for Scattering by Two and Three Dimensional Structures," to be presented at the 1990 URSI General Assembly, Session B4, Prague, Chechoslovakia; Conference Proceedings p. 384.
15. M.A. Ricoy and J.L. Volakis, "On the Analytical Implementation of Generalized Impedance Boundary Conditions," to be presented at the 1990 URSI General Assembly, Session B5, Prague, Chechoslovakia; Conference Proceedings p. 391.
16. J.M. Jin and J.L. Volakis, "A Finite Element-Boundary Integral Formulation for Scattering by A Three Dimensional Aperture in a Thick Conducting Plane," Submitted to the 4th Biennial IEEE Conference on Electromagnetic Field Computation, Oct. 1990, Toronto.
17. M.A. Ricoy and J.L. Volakis, "Diffraction by Material Junctions," Journess Internationales De Nice Sur Les Antennes (JINA), Nov. 1990, Nice France; Conference Proceedings pp. 34-44.

REPORTS WRITTEN TO DATE UNDER THIS GRANT

J.L. Volakis, T.B.A. Senior and J.-M. Jin, "Derivation and Application of a Class of Generalized Impedance Boundary Conditions - II," University of Michigan Radiation Laboratory, Technical Report 025921-1-T, February 1989, 47 pp.

K. Barkeshli and J.L. Volakis, "Scattering by a Two-Dimensional Groove in a Ground Plane," University of Michigan Radiation Laboratory, Technical Report 025921-2-T, February 1989, 31 pp.

H.H. Syed and J.L. Volakis, "An Approximate Skew Incidence Diffraction Coefficient for an Impedance Wedge," University of Michigan Radiation Laboratory, Technical Report 025921-4-T, September 1989, 31 pp.

M.A. Ricoy and J.L. Volakis, "Derivation of Generalized Transition/Boundary Conditions for Planar Multiple Layer Structures," University of Michigan Radiation Laboratory, Technical Report 025921-5-T, September 1989, 36 pp.

M.A. Ricoy and J.L. Volakis, "Diffraction by a Multilayered Slab Recessed in a Ground Plane via the Generalized Impedance Boundary Conditions," University of Michigan Radiation Laboratory, Technical Report 025921-8-T, Dec. 1989, 43 pp.

H.H. Syed and J.L. Volakis, "An Asymptotic Analysis of the Plane Wave Scattering by a Smooth Convex Impedance Cylinder," University of Michigan Radiation Laboratory, Technical Report 025921-9-T, Jan. 1990. 31pp.

M.A. Ricoy and J.L. Volakis, "Electromagnetic Scattering from Two-Dimensional Thick Material Junctions," University of Michigan Radiation Laboratory 025921-14-T, August 1990. 166 pp.

H.H. Syed and J.L. Volakis, "High Frequency Scattering by a Smooth Coated Cylinder Simulated with Generalized Impedance Boundary Conditions," University of Michigan Radiation Laboratory Report 025921-17-T, January 1991. 32 pp.

J.L. Volakis, "Semi-Annual Progress Report for NASA Grant NAG-2-541," The University of Michigan Radiation Laboratory, Technical Report 025921-3-T, 45 pp.

J.D. Collins and J.L. Volakis, "A Combined Finite Element and Boundary Integral Formulation for Solution via CGFFT of Two-Dimensional Scattering Problems," University of Michigan Radiation Laboratory, Technical Report 025921-6-T, September 1989, 73 pp.

J.L. Volakis, "Semi-Annual Report for NASA Grant NAG-2-541," University of Michigan Radiation Laboratory, Report 025921-7-T, September 1989, 46 pp.

J.M. Jin and J.L. Volakis, "A Finite Element-Boundary Integral Formulation for Scattering by Three-Dimensional Cavity Backed Apertures," University of Michigan Radiation Laboratory Technical Report 025921-10-T, February 1990. 28 pp.

J.D. Collins, J.M. Jin and J.L. Volakis, "A Combined Finite Element-Boundary Element Formulation for Solution of Two-Dimensional Problems via CGFFT," University of Michigan Radiation Laboratory Technical Report 025921-11-T, February 1990. 45 pp.

J.L. Volakis, "Semi-Annual Report for NASA Grant NAG-2-541, "University of Michigan Radiation Laboratory Report 025921-12-T, February 1990. 60 pp.

J.L. Volakis, "Semi-Annual Report for NASA Grant NAG-2-541, "University of Michigan Radiation Laboratory Report 025921-13-T, September 1990. 56 pp.

C. Hua, "Users Manual for AUTOMESH-2D A Program of Automatic Mesh Generation for Two-Dimensional Scattering Analysis by the Finite Element Method," University of Michigan Radiation Laboratory Report 025921-15-T, August 1990, 38 pp.

J. Zapp, "Examples of Finite Mesh Generation using SDRC IDEAS," University of Michigan Radiation Laboratory Report 025921-16-T, September 1990, 52 pp.

J.D. Collins and J.L. Volakis, "A Combined Finite Element-Boundary Element Formulation for Solution of Axially Symmetric Bodies," University of Michigan Radiation Laboratory Report 025921-18-T, January 1991. 64 pp.

